Project Number: ME-CAB-1602

Correlating Shoe Sole Surface Roughness to Coefficient of Friction

A Major Qualifying Project Report:

submitted to the Faculty

of the

WORCESTER POLYTECHNIC INSTITUTE

in partial fulfillment of the requirements for the

Degree of Bachelor of Science

In Mechanical Engineering

by

Brien F. Hard

Joseph F. Lidwin

Christopher H. Murray

Date: 28 April 2016

Approved:

_____

Prof. Christopher A. Brown, Major Advisor

Abstract

This project evaluated the feasibility of correlating surface roughness to coefficient of friction on a shoe sole's polymer-based material. We used state of the art microscopes to measure the surface of polymer compounds at fine scales. We used geometric multiscale analysis to characterize the surface and determine the relevant scales of measurement. We designed a testing device that can apply a measurable normal and transversal force at the interaction of two surfaces. We used a dynamometer to measure the two forces simultaneously to calculate the coefficient of friction. This study demonstrated that with a more diverse selection of surface topographies one should be able to find a correlation.

Table of Contents

Table of Figures

Table of Tables

Foreword

Much of this project was done in close conjunction with Connor King who wrote Correlating Shoe Sole Friction to Surface Roughness. This collaboration includes many aspects of the design work, procedure development, testing, and writing. There is a great deal of overlap between our introduction, data, and write up.

Acknowledgements

We would like to thank the following people for their contributions to our project:

Professor Christopher A. Brown, WPI

Steve Ellis, Vibram

Isabel Pagliaccio, Vibram

Connor King, WPI

WPI Surface Metrology Laboratory Staff

1. Introduction

1.1 Objective

The objective of this project is to determine a correlation between coefficient of friction (COF) and the surface roughness of a shoe sole against a counter surface. This project will involve designing a testing procedure to determine the COF and using the multi-scale geometric analysis method to characterize a surface's roughness in an attempt to find the relationship between the two.

1.2 Rationale

More than 37 million slip and falls occur each year during recreational, work, and daily activities (WHO 2012). Studies have found that friction is the most critical factor in the occurrence of a slip and fall (Way 2006). An understanding of COF and how different surfaces interact would provide shoe makers with a better understanding on how to improve the COF of shoe soles on concrete, hardwood flooring, carpet, and other recreational and workplace surfaces. Using state of the art methods we will be able to analyze factors that affect the COF which previous standardized testing does not address. Providing a direct relationship between surface roughness and the COF can provide manufacturers with information to help understand how their shoe will behave on surfaces in certain conditions.

1.3 State of the Art

Measuring the coefficient of friction involves the interaction between two surfaces. To fully understand the COF measurement, the surface roughness properties of both surfaces needs to be analyzed. Through the use of ASTM, ASME, and ISO standards, surface roughness can be measured and characterized to establish parameters, such as peak height or roughness average, that most significantly influence the COF between a shoes' sole and counter surface. Establishing a strong understanding of surface roughness and having accurate COF measurements is the basis for being able to determine a correlation between the shoe sole and counter surface.

1.3.1 Surface Roughness

Surface roughness is generally measured by taking the average height of the surface over the length of the surface, R_a. The length of the surface is determined by the cutoff wavelengths which the user defines. Other parameters have been used to characterize surface roughness over a given length which include slope, root mean square, and maximum profile height. These parameters are used to help determine how surface roughness affects different tribological phenomena. ASME standard B46.1 helps better explain surface texture parameters and how they are used to characterize surface roughness.

Another method for characterizing surface roughness is multi-scale geometric analysis. This method utilizes a confocal microscope to analyze the texture of a surface at different measurement scales. The texture area is then broken down into partitions of geometric shapes based on the scale. It also simplifies the process of correlating common surface roughness parameters outlined in ASME B46.1 and the different measurement scales of the surface. The best scale for measuring the surface is found by finding which scale produces the best R(squared) values for the parameter.

Case Study 1: How to select the most relevant 3D roughness parameters of a surface

In a study on "How to select the most relevant 3D roughness parameters of a surface," Deltombe et al. detail a process for determining the relevance of measured surface topography values. The first step is to take measurements of various surface roughness parameters. For this study a white light interferometer was used for "characterizing and quantifying surface roughness." The second step is is a multiscale decomposition, which uses a Gaussian filter, as recommended by ISO and ASME standards, to determine the mean line of the surface metrology. From these measurements taken at varying scales various 3D roughness parameters are computed. Step three is to use a statistical model to measure the variance and thus the relevancy of each parameter for each spatial scale. The final steps in the process are to classify each parameter, determine which are most relevant and interpret the physical ramifications of each. This study details an "elementary study of surface topography" (Deltombe et al. 2014).

Case Study 2: Floor slipperiness measurement: friction coefficient, roughness of floors, and subjective perception under spillage conditions

Another study, carried out by Li et al. set out to understand the "risk of slipping accidents." This study tested five common floor materials for their COF with four common shoe materials under five different spill conditions. The researchers first measured the surface roughness of the tiles using a profilometer to measure for four surface roughness parameters (R_a, R_{tm}, R_{pm}, and R_q). Then COF was measured by using a Brungraber Mark II COF tester which simultaneously applies the normal and transversal forces. A weighted inclined strut impacts the counter surface at specified angle, the angle is increased until a slip occurs in which the tangent of the angle is the COF. The COF data and the surface roughness data were then plotted against each other. The results attained were a "very high (r=0.932 to 0.99)" correlation. This study is an example of research that was able to attain very good correlation results (Li et al. 2004)

1.3.2 Friction

Several standards currently exist to test the dynamic coefficient of friction between the shoe sole and counter surface. The British standard BS 7976-2:2002 + A1:2013, which was amended in 2013, outlines the methods for establishing a pendulum shoe friction test. This standard provides useful information about procedures currently used for testing shoe sole

friction. Other standards include EN ISO 13287:2007 and ASTM F2913-11 which specify methods for testing the COF of shoe soles by manipulating the properties of the counter surface.

To understand the coefficient of friction between shoe and counter surface, "standardized mechanical test devices have been developed to simulate dynamic footwear-surface interaction to provide a repeatable measure of floor slipperiness." (Clark et al 2015). A pendulum testing machine and a SATRA STM 603 machine are currently used for testing friction as it relates to shoe soles. The pendulum testing machine uses a pendulum like motion to move and measure the displacement of the shoe sole as it comes into contact with the surface. The procedures and methods for using the pendulum testing machine are outlined in the BS 8976-2:2002 +A1:2013 standard. The SATRA STM 603 machine is a slip resistance testing device to test the friction of the shoe sole-counter surface interface. The company SATRA is an independent research and testing organization that developed the test to follow the EN ISO 13287:2007 standard. Additionally, the organization established its own standard SATRA TM144 which can be read to better understand the testing procedure and methods. All of the standards that are relevant and studied for purposes of this project can be found in Table 1.

Standards for Testing Coefficient of Friction for Shoe Soles	
EN ISO 13287:2007	specifies methods for testing for the slip resistance of conventionally soled safety
ASTM F2913-11	specifies method for measuring the coefficient of friction of shoe soles using a whole shoe tester
BS 7976-2:2002 + A1:2013	outlines methods for measuring coefficient of friction of shoe soles using a pendulum tester
SATRA TM144	specifies methods for testing coefficient of friction of shoe soles using STM 603 machine

Table 1: Standards for testing coefficient of friction for shoe soles

This study analyzed the factors that influenced the COF on shoe soles. Derler et al investigated the factors that influenced the results of the friction measurement by using a tribometer Floor Slide Control 2000 that was operated under different condition in a climate chamber. The device was operated over a specified distance and velocity to measure the dynamic coefficient of friction between a standard material to mimic a shoe sole such as rubber, plastic or leather and the underlying surface, either PVC flooring of terrazzo tiles. Each combination was carried out under four different temperatures. From there the hardness of all shoe sole materials were measured under the different temperatures. After all the measurements and trials were carried out they were able to analyze the data through software Mathematica® (Wolfram, 1996)

and statistical methods described in Sachs (2004). This study showed a simple slip resistance test while taking into consideration the temperature effect on the COF on the shoe sole materials. While the friction that was measured was a result of the viscoelastic material properties and depended on the hardness of the shoe sole, the temperature and mechanical abrasion of the sole materials were the two factors with the greatest effect on the dynamic COF.

Case Study 4: Understanding the Friction Measured by Standardized Test Methodologies Used to Assess Shoe-Surface Slip Risk

Currently there are two shoe-surface contact testing methods that assess the risk of a pedestrian slip specified in British Standards. There is the aforementioned BS 7976-2:2002 pendulum test device and BS EN ISO 13287:2007 which specifies the test method to assess the slip resistance of conventionally soled safety, protective and occupational footwear. In this study experiments were conducted on six different household surfaces. The results showed no correlation between the two standardized test methods. Clark et al believe this can be attributed to the effect that the different methodologies have on the friction factors at the heel-surface contact. The results do suggest that a linear relationship between roughness and slip resistance may exist for stiff surfaces however the relationship does not include deformed surface. "With stiff surfaces, the friction caused by asperity contact is dominant and controlled by surface roughness" (Clark et al 2015).

1.3.3 Correlation

Using the methods and standards for characterizing surface roughness and measuring the coefficient of friction, a correlation between the two can be determined. Most often, surface roughness and COF are correlated through the use of linear regression analysis. This method for correlation was used in a study from 2010 analyzing milled steel die surface roughness correlation with steel sheet friction (Berglund et al 2010). Linear regression analysis produces an equation that can determine a y-value given an x-value. For this research, the surface roughness parameter is the x-value used to determine the COF (y-value). This method also creates a value, R^2, which determines the strength of correlation. A value of 1 is ideal as it means that it is a perfect correlation.

Case Study 5: Milled Die Surface Roughness Correlation

In a study on milled die steel surface roughness correlation with steel sheet friction, a team of engineers conducted linear regression analysis of 32 characterization parameters against the surface roughness of milled die. The purpose of performing the analysis was to determine which characterization parameters best relates the friction found in sheet metal forming and the surface roughness of metal dies. The study used the bending under tension test of sample surfaces, a test commonly used when analyzing metal dies, to measure friction. Through the use of linear regression analysis, the study was able to compare the friction measurements against the surface parameters by producing R^2 values and was able to determine which parameters were

most closely related to the friction found in sheet metal forming. This study exhibits a good example of how a linear regression analysis can be useful in relating factors of surface roughness with friction. The study was able to find that inclinations of a surface roughness are important to consider when analyzing friction in sheet metal forming because of their strong correlation factor. The study also provides a good example of how to understand the linear regression models that the analysis produces to determine which parameters should be considered and which should not be considered (Berglund et al 2010).

1.4. Approach

To satisfy the goal of finding the correlation between the surface roughness and COF we will break the project up into three areas of work: designing a process to characterize surface roughness of a shoe sole and counter surface, designing a system to simultaneously measure the forces to determine the COF, and analyzing the results to determine the correlation.

The project team will utilize axiomatic design for the duration of this project for any aspect that requires design. By using axiomatic design the project team will ensure that its work is as effective and accurate as possible. Finally it will also help the team to develop important insight and ideas related to the projects designs, testing, and analysis.

1.4.1 Surface roughness of shoe sole and counter surface

This project's objective is different from previous studies such as case study 2 in the "state of the art" section because it specifically deals with the correlation between two objects surface roughness and the resulting COF. Understanding the scale of interaction of the surfaces helps to better understand how the selected parameters relate to the properties of the roughness of the surface. As a result we will use the multi-scale geometric analysis for the shoe sole surface as well as common floor surfaces used in shoe testing. A list of the common floor surfaces can be found in Table 2. The method of multi-scale geometric analysis has not been used in past studies to identify a relationship between surface roughness and the COF of a shoe sole and a counter surface.

Common Counter Surfaces
Unglazed clay quarry tile
Stainless steel number 1.4301 type 2G
Vinyl (PVC)
Wood
Carpet
GRP
Concrete

Table 2: Common counter surfaces used in shoe testing

1.4.2 Simultaneous measurement of forces

Once the roughness of the surface and the significant parameters are determined, a better understanding of the relationship with the COF measurement may be accomplished. When measuring the COF, it is important to measure both the tangential and normal forces at the same time. To do this, a Kistler dynamometer, which is capable of quasi-static and dynamic measurements, can be used to measure the forces simultaneously. The tangential forces of friction directly impact the normal forces of friction, therefore if the two forces are not measured simultaneously than a clear picture of the coefficient of friction cannot be understood. This process is different from the approach used in studies such as case study 3 which uses a portable device to measure slip resistance. The Kistler dynamometer will provide our team will real time data of both forces during static and dynamic friction testing instead of a device automatically calculating the COF. Measuring the forces simultaneously and establishing a scale with significant parameters for surface roughness will give us a better picture to correlate coefficient of friction with surface roughness.

1.4.3 Determine the correlation

The most accurate approach that will provide the most incite whether there is a correlation between the COF and the surface roughness of a shoe sole against a contact surface is a linear regression analysis. This method is discussed in case study 5.

2. Methods

2.1 Friction Measurement

2.1.1 Testing Materials

2.1.1.1 Polymer Bases

To assess polymer samples of shoe soles currently used in production, Vibram was able to provide us with the polymer samples used in this project. For more information on the polymer samples refer to Appendix A.

2.1.1.2 Rapid Prototyped Block

Due to the thickness of the material, 3.63 mm (0.143”), we designed a spacer that would enable us to apply and control the normal and tangential forces to the material. For more information on our spacer refer to Appendix B.

2.1.2 Kistler Dynamometer

Forces in the normal and tangential directions affect the COF. A common method for measuring COF is to calculate the forces individually and then average the ratios. The average of the ratios is different from the ratio of the average. This means that the average of the ratio of normal force calculations and ratio of tangential force calculations does not produce the same result as the ratio of the average normal and tangential calculations. Taking the ratio of the averages provides a more precise COF measurement as both forces affecting it are calculated simultaneously. The project used a Kistler dynamometer to measure the forces simultaneously. For more information on the dynamometer and how it works refer to Appendix C. For more in-depth information on the friction measurement set-up and process refer to Appendix D.

2.1.3 Friction Measurement Procedure

To determine the COF of the rubber sample, we designed a system that could apply a force in the normal and tangential directions on the material. For more information on our procedure refer to Appendix E.

2.2 Surface Metrology

2.2.1 Surface Measurement

To analyze the surface of the polymer samples, we used an Olympus LEXT OLS 4100 confocal microscope. The microscope measures the topography of our material at 10 nanometer resolutions. The microscope’s nanometer resolution was needed to obtain surface measurements since the surfaces used were optically smooth. For information on how we prepared and measure the material refer to Appendix F.

2.2.2 Use of MountainsMap

MountainsMap is a program developed by Digital Surf with the capability to interpret and analyze measurements taken by the Olympus microscope. There were three possible areas that could affect the result of our surface roughness parameters that our team analyzed to get an average roughness value. For more information on how we filtered the material in MountainsMap refer to Appendix G.

2.2.3 Correlation

2.2.3.1 Surface Roughness and Volume Parameter Correlation

Previous case studies concluded that some conventional surface roughness parameters show strong correlation to tribological phenomena. These parameters include max peak height (Sp), minimum depth of valleys (Sv), maximum surface height (Sz), arithmetic average (Sa), and root mean square roughness (Sq). We also tested volume parameters such as material volume (Vm), peak material volume (Vmp), and core material volume (Vmc). It is important to measure these conventional parameters to determine if there is a possible correlation with the COF measurements.

After we took a measurement of the surface from the Olympus microscope, MountainsMap can extract the value of these parameters. The parameters along with the COF values are put into an Excel spreadsheet. Excel has the ability to perform linear and second degree order regression analysis to calculate an R^2 value. The R^2 value represents how close the values in a given data set are to the equation of the regression line calculated in the regression analysis. The closer the R^2 value is to 1.0, the closer the data points are to the regression line.

2.2.3.2 Sfrax

Multiscale geometric analysis is a method for interpreting the relative area of a surface at various scales of observation. The method takes a surface's area and breaks it down into partitions of geometric shapes based on the scale. The larger the scale, the larger the partitions of geometric shapes. The partitions help to provide data for the relative area of the surface. This data is analyzed with COF measurements to determine if a correlation exists.

We used the software Sfrax to perform the multi-scale geometric analysis. A WPI student designed the program to read surface measurements and perform area-scale analysis. The process we used in performing the analysis was to import our stitched surface measurements into Sfrax. The area-scale analysis and four corners and full overlap method was performed on the surface measurements to produce data on the relative area of the surface at a range of scales.

Sfrax also has the capability to allow the user to input surface properties, such as COF, in order to perform a linear regression analysis. This function was used to determine if a correlation existed between a surface's relative area and COF measurements.

3. Results

3.1 COF Measurements

3.1.1 Dynamometer Measurements

Through the use of the VI program designed in LabView, we were able to produce graphs for our COF measurements. Below are Figures 1 and 2 which show the data we received for two different trials.

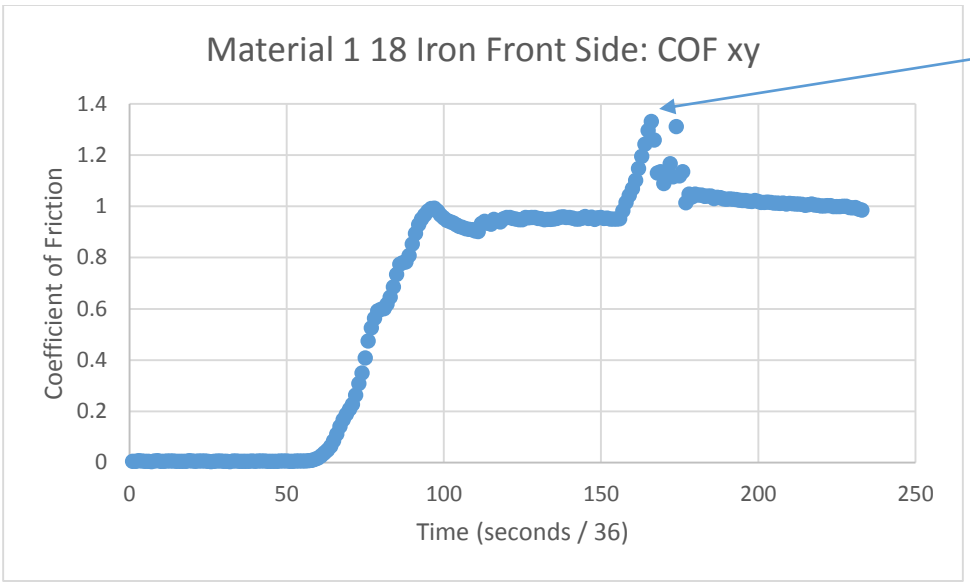

Figure 1: COF Data for Material 1 18 Iron Front Side

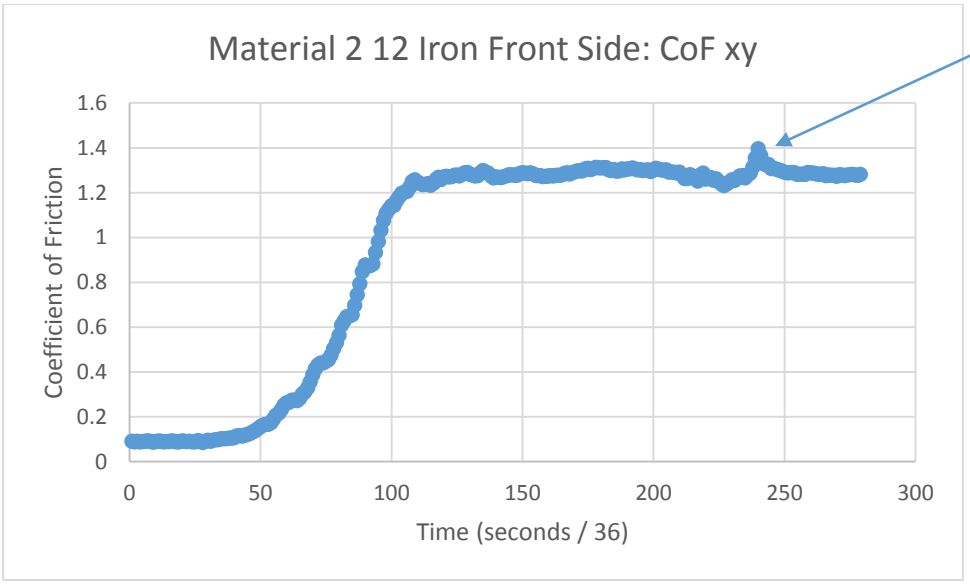

Figure 2: COF Data for Material 2 12 Iron Front Side

The first increase in the figures above, from zero to about one, represent the lowering of the weight on the pulley. For all of the trials the hanging weight was not enough force to make the material move on the counter face. The flat line in the figures from time 100 to 150 represents this. We then had to apply a small additional force to the rope. We did this by applying a slow pull of the rope where we increased the force of the pull until the block moved. The peak of the graph at time 165 represents when the block exceeded the static COF. The peak value was the value we used as the COF measurement for that trial. For each surface we performed six trials. We took the average of each trial's peak to obtain the average COF measurement of the surface. We followed this same procedure for each of our surfaces. Table 3 shows the average COF values for each surface.

Material	COF	Std Dev
Spec 1 18 Iron Frontside	1.384878	0.053186
Spec 1 12 Iron Frontside	1.590392	0.099352
Spec 1 ASTM Backside	1.369278	0.14118
Spec 1 ASTM Frontside	1.448452	0.158926
Spec 2 ASTM Frontside	1.539579	0.061997
Spec 2 ASTM Backside	1.789609	0.041101
Spec 2 12 Iron Frontside	1.35968	0.054769
Spec 2 18 Iron Frontside	1.293991	0.052835

Table 3: Average COF for Tested Materials

3.2 Surface Measurements

3.2.1. Height and Volume Parameters

The stitched surfaces for both material one and material two produced conventional surface height and volume parameters to determine if a correlation existed between these parameters and the COF. We used the program MountainsMap to determine these parameters.

Material	Height Parameters					Volume Parameters				COF	Std Dev
	Sq	Sp	Sv	Sz	Sa	Vmp	Vmc	Vvc	Vvv		
Spec 1 18 Iron Frontside	2.13	6.71	14	20.7	1.67	0.0808	1.86	2.23	0.316	1.384878	0.053186
Spec 1 12 Iron Frontside	3.09	8.99	11.7	20.7	2.44	0.145	2.61	3.94	0.346	1.590392	0.099352
Spec 1 ASTM Backside	1.67	5.85	6.37	12.2	1.33	0.0821	1.53	1.89	0.201	1.369278	0.14118
Spec 1 ASTM Frontside	1.53	20.8	13	33.7	1.22	0.0771	1.38	1.88	0.171	1.448452	0.158926
Spec 2 ASTM Frontside	1.6	6.36	6.22	12.6	1.27	0.0699	1.44	2.01	0.184	1.539579	0.061997
Spec 2 ASTM Backside	1.59	5.16	6.26	11.4	1.25	0.0701	1.45	1.81	0.203	1.789609	0.041101
Spec 2 12 Iron Frontside	2.55	10.7	11.5	22.2	1.99	0.105	2.07	3.08	0.347	1.35968	0.054769
Spec 2 18 Iron Frontside	3.93	14.8	18.6	33.4	3.14	0.138	3.58	4.74	0.477	1.293991	0.052835

Table 4: Values of the surface height and volume parameters for all of the surfaces.

3.3 Correlation Results

3.3.1 Excel Correlations

We used Microsoft Excel to calculate the linear regression analysis for the conventional height and volume parameters. Similar to when we calibrated the dynamometer, we put the values of the parameters and COF in an Excel spreadsheet. We plotted the surface parameters for the surfaces of each material against their COF values in a scatterplot. Excel has the function to calculate the linear regression equation and R^2 value to determine correlation. As stated in the methods, the closer the R^2 value is to 1 the greater influence the parameter has on the COF value. Figure 3 shows the Excel scatterplot, linear regression equation, and R^2 value for max peak height vs COF for material 2.

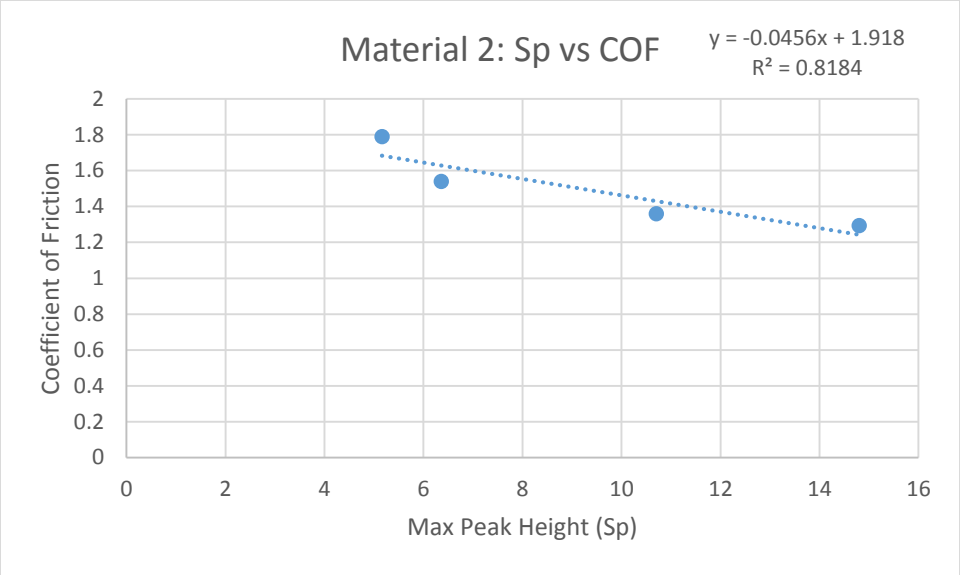

Figure 3: Sp vs COF Correlation of Material 2

Figure 4 shows the Excel scatterplot, linear regression equation, and R^2 value for peak material volume for material 1.

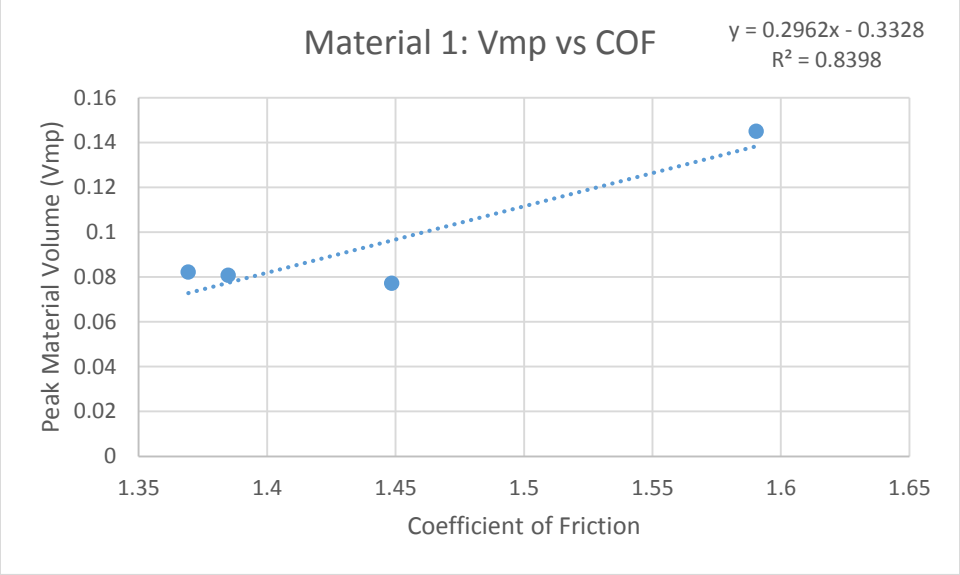

Figure 4: Vmp vs COF Correlation of Material 1

Table 5 shows the full list of results for the R^2 values of the volume and height parameters. We explain all the parameters and what they mean in method 2.2.3.1.

Material	Modulus of Elasticity	Volume Parameters				Height Parameters				
		Vmp	Vmc	Vvc	Vvv	Sq	Sp	Sv	Sz	Sa
1	7.042×10^6	0.8398	0.8238	0.8238	0.2656	0.6566	0.0355	0.0719	0.0631	0.6687
2	4.899×10^6	0.7222	0.5894	0.7161	0.6891	0.6721	0.8184	0.6786	0.7422	0.6635

Table 5: Correlation Values for Volume and Height parameters

3.3.2 Relative Area vs Scale Analysis

To perform multi-scale geometric analysis, our team used SFrax to perform area-scale analysis. The results shown in Figure 5 show the relative area at multiple scales for material 1.

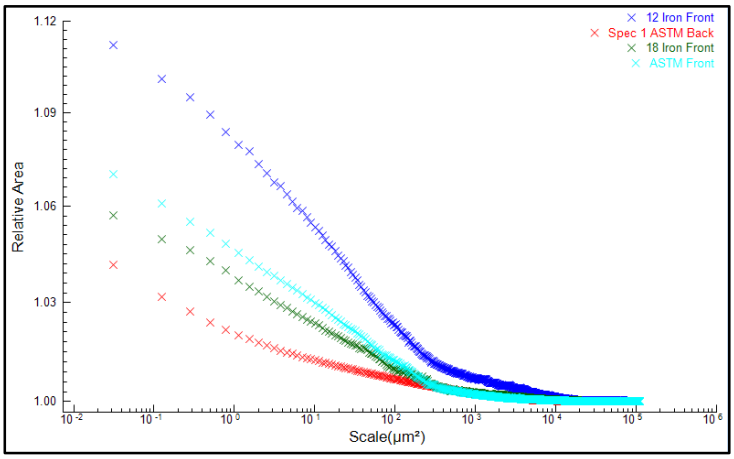

Figure 5: Relative Area vs Scale for Material 1. Dark Blue line is the 12 Iron Surface, Light Blue line is the ASTM Front Surface, Green line is the 18 Iron Surface, and the Red line is the ASTM Back Surface

This figure helps to illustrate at what scale we can distinguish between the four surfaces we measured for material 1. Based on this figure, the surfaces are undistinguishable from 10^5 µm^2 to 10^3 µm^2. At 10^3 µm^2 the 12 iron front side surface begins to become distinguishable from the other three surfaces and by 90 µm^2, all four surfaces become distinguishable from each other. This is important when analyzing the regression analysis because the values that will show us how the surfaces correlate will be from 90 µm^2 and smaller.

Figure 6 shows the relative area at multiple scales for material 2.

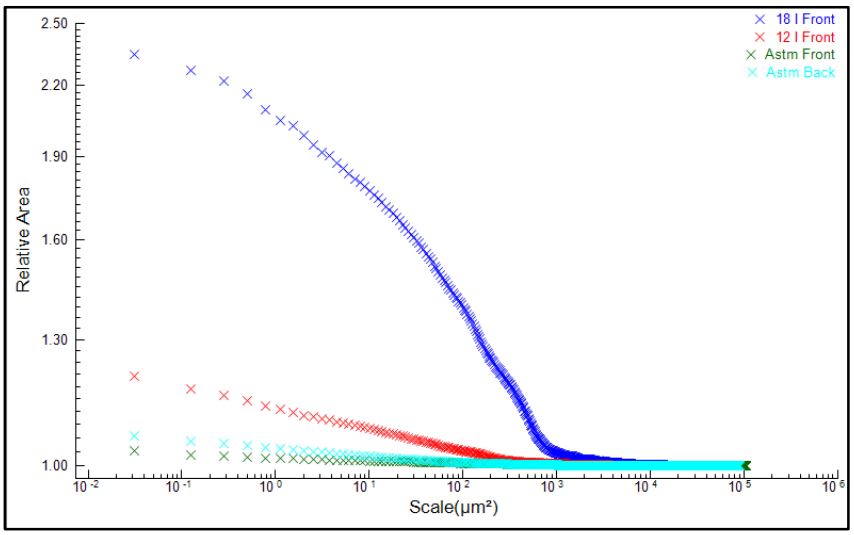

Figure 6: Relative Area vs Scale for Material 2. Dark Blue line is the 18 Iron Surface, Red line is the 12 Iron Surface, Light Blue is the ASTM Back Surface, Green line is the ASTM Front Surface

Figure 6 helps to illustrate at what scale we can distinguish between the four surfaces we measured for material 2. Based on this figure, the surfaces are undistinguishable from 10^5 µm^2 to 10^3

μm^2. At 10^3 μm^2 the 18 iron front side surface begins to become distinguishable from the other three surfaces and by 70 μm^2, all four surfaces become distinguishable from each other. This is important when analyzing the regression analysis because the values that will show us how the surfaces correlate will be from 80 μm^2 and smaller.

3.3.3 Relative Area Regression Analysis

We used the SFrax variable correlation tool to calculate the R^2 value between relative area and COF. Figure 7 shows the plot of R^2 values vs scale for material one.

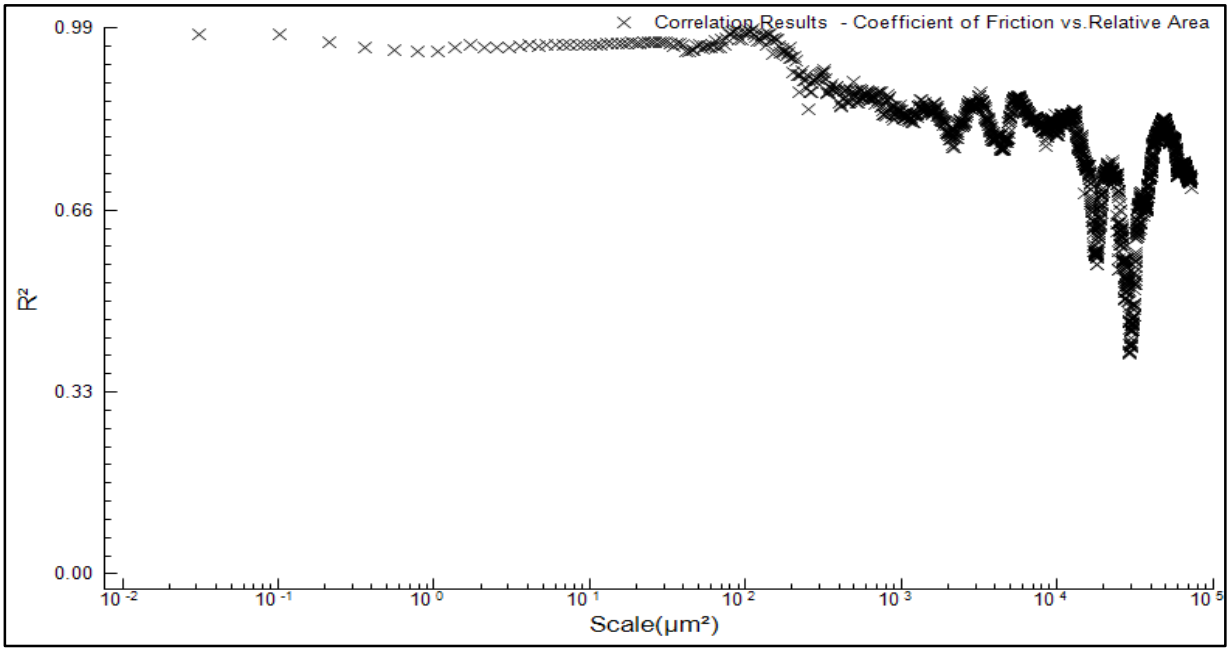

Figure 7: Correlation results of Relative Area and COF of Material 1

Figure 7 helps to illustrate how well the relative area of the material one surfaces correlates with the COF measurement of the surface. From Figure 7, we understand that the R^2 values from 10^5 μm^2 to 10^3 μm^2, possibly fluctuate due to high peaks or irregularities of one of the four surfaces because the four surfaces cannot be distinguished. From a scale of 90 μm^2 and smaller, we see that there is a consistent R^2 value of 0.99. This indicates that 99% of the variation in COF measurements for material one are due to the relative area of the surface. This means that there is a close correlation between surface roughness and coefficient of friction for material 1.

Figure 8 shows the plot of R^2 values vs scale for material 2.

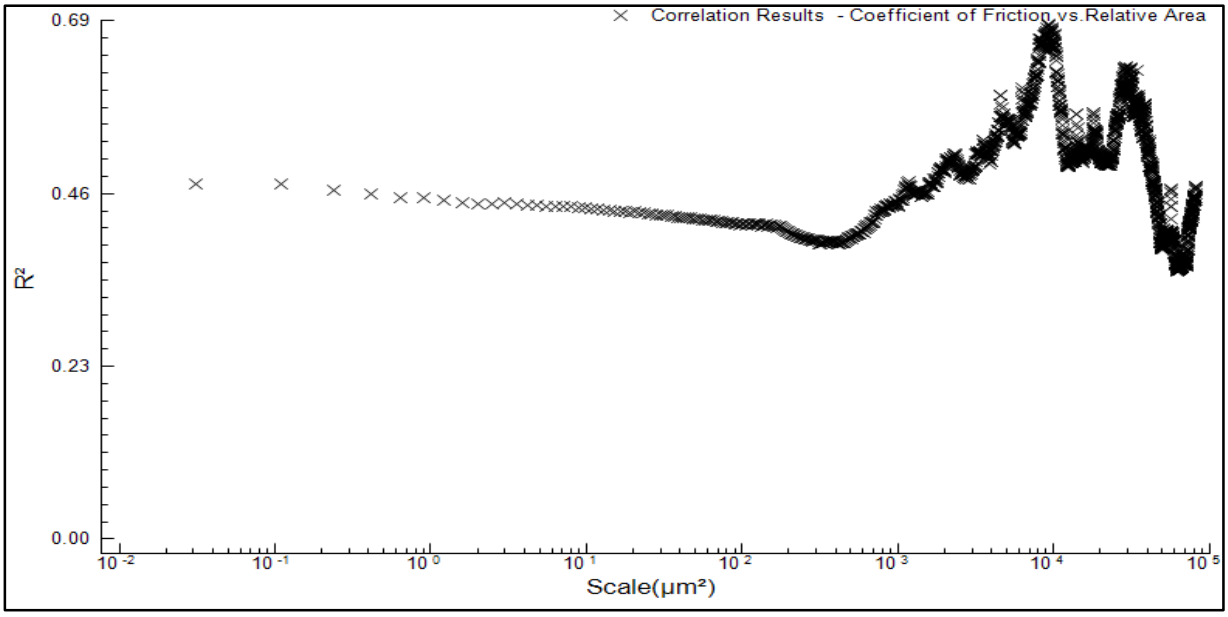

Figure 8: Correlation results of Relative Area and COF of Material 1

Figure 8 helps to illustrate how well the relative area of the material two surfaces correlates with the COF measurement of the surface. From Figure 8, we understand that the R^2 values from 10^5 μm^2 to 10^3 μm^2, possibly fluctuate due to high peaks or irregularities of one of the four surfaces because the four surfaces cannot be distinguished. From a scale of 70 μm^2 and smaller, we see that there is a consistent R^2 value of 0.47. This indicates that 47% of the variation in COF measurements for material one are due to the relative area of the surface. This means that there may be a correlation between surface roughness and coefficient of friction for material 2.

3.3.4. Complexity vs Scale Analysis

To perform multi-scale geometric analysis, our team used SFrax to perform complexity-scale analysis. The complexity is the scale based derivative of the relative area of the surfaces. Mathematically, the complexity is the slope of the relative area over one decade. For purposes of this project, this helps us understand what is going on with the correlation between surface roughness and COF at each decade. On the surface, if there are multiple large peaks at the large scales the entire surface will be characterized by those peaks in a relative area analysis. The complexity scale helps to eliminate this by taking the average surface measurement at fine scales. This allows us to analyze the average roughness instead of a measurement characterized by a few large peaks that may exist. The results shown in Figure 9 show the complexity at multiple scales for material one.

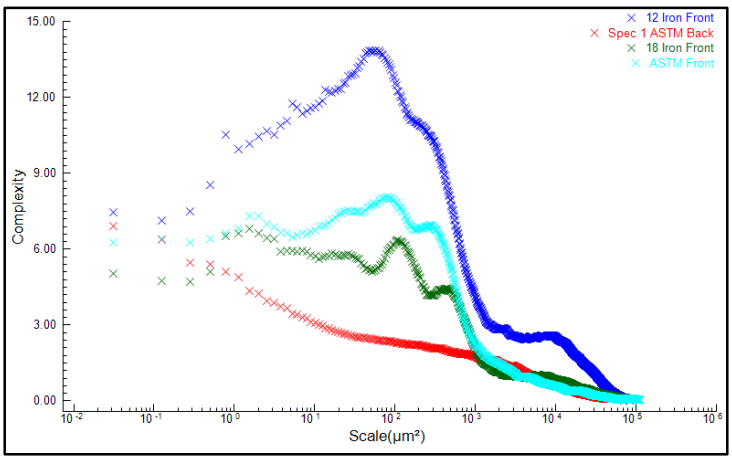

Figure 9: Complexity vs Scale for Material 1 Surface Measurements. Dark Blue line is the 12 Iron Surface, Light Blue line is the ASTM Front Surface, Green line is the 18 Iron Surface, and the Red line is the ASTM Back Surface

This figure helps to illustrate at what scales we can distinguish between the complexities of the four surfaces we measured for material one. Based on this figure, the surfaces are undistinguishable from 10^5 µm^2 to 10^3 µm^2. At approximately 700 µm^2 the four surfaces become distinguishable from each other. This is important when analyzing the regression analysis because the values that will show us how the surfaces correlate will be from 700 µm^2 and smaller.

Figure 10 shows the complexity at multiple scales for material two.

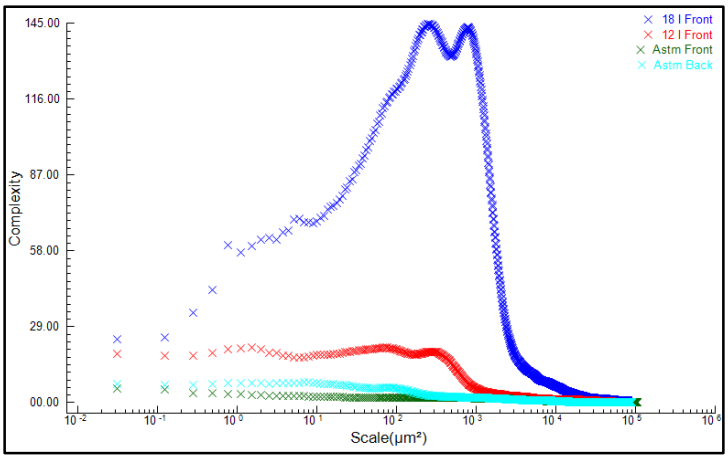

Figure 10: Complexity vs Scale for Material 2 Surface Measurements. Dark Blue line is the 18 Iron Surface, Red line is the 12 Iron Surface, Light Blue is the ASTM Back Surface, Green line is the ASTM Front Surface.

This figure helps to illustrate at what scales we can distinguish between the complexities of the four surfaces we measured for material two. Based on this figure, the surfaces are undistinguishable from 10^5 µm^2 to 10^2 µm^2. At approximately 90 µm^2 the four surfaces become distinguishable from each other. This is important when analyzing the regression analysis because the values that will show us how the surfaces correlate will be from 90 µm^2 and smaller.

3.3.5. Complexity Regression Analysis

We used the SFrax variable correlation tool to calculate the R^2 values between complexity and COF. Figure 11 shows the plot of R^2 values vs scale for material one.

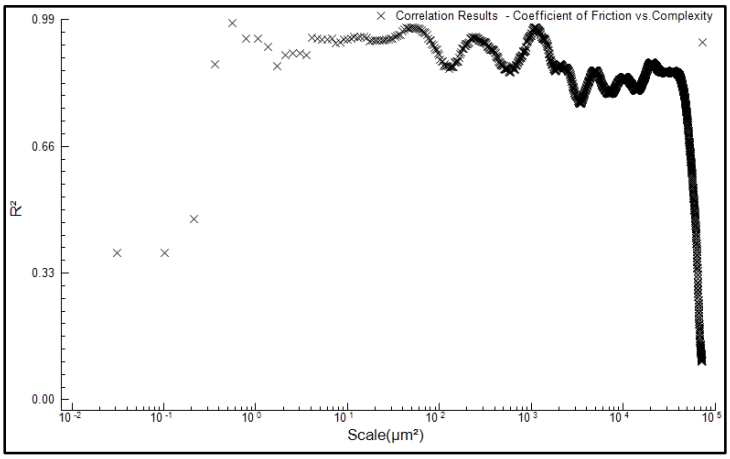

Figure 11: Regression Analysis of Complexity vs COF of Material 2

Figure 11 helps to illustrate how well the complexity of the material one surfaces correlates with the COF measurement of the surface. From Figure 11, we understand that the R^2 values from 10^5 μm^2 to 10^3 μm^2, possibly fluctuate due to high peaks or irregularities of one of the four surfaces because the four surfaces cannot be distinguished. From a scale of 700 μm^2 to about 9 μm^2, we see that there is a consistent R^2 value of 0.99. This indicates that 99% of the variation in COF measurements for material one are due to the complexity of the surface. This means that there is a close correlation between surface roughness complexity and coefficient of friction for material one. From about 9 μm^2 and smaller we see a fluctuation from the .99 R^2 value. This may be explained by the change in complexity of the 18 Iron front side surface that drops below the ASTM back side surface complexity in this scale range.

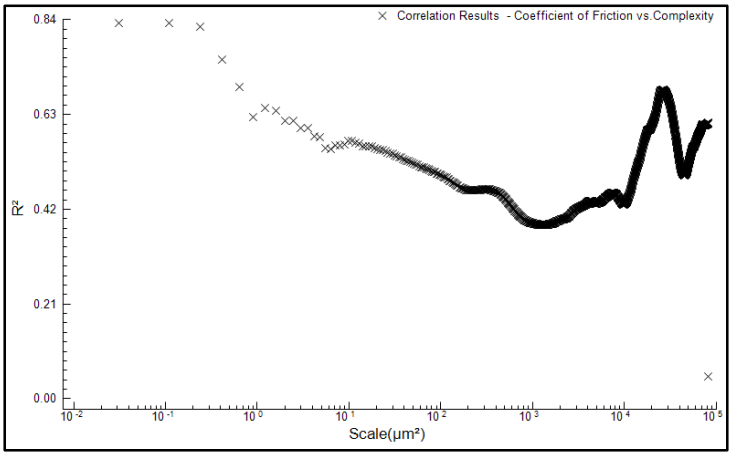

Figure 12: Regression Analysis of Complexity vs COF of Material 2

Figure 12 helps to illustrate how well the complexity of the material two surfaces correlates with the COF measurement of the surface. From Figure 12, we understand that the R^2 values from 10^5 μm^2 to 10^2 μm^2, possibly fluctuate due to high peaks or irregularities of one of the four surfaces because the four surfaces cannot be distinguished. From a scale of 90 μm^2 to 10 μm^2 we see a steady incline in R^2

that leads up to a peak R^2 value of 0.58. This indicates that 58% of the variation in COF measurements for material two are due to the complexity of the surface. From approximately 7 μm^2 and smaller, the fluctuation in the R^2 value may be due to the decrease in complexity of the 18 Iron front side surface. This means that there may be a correlation between surface roughness complexity and coefficient of friction for material two.

4. Discussion

4.1 Friction Testing

We attempted to design a testing device that would enable us to measure how much force we were applying in the normal and tangential directions on the dynamometer. Axiomatic design was the primary design process in order to manufacture a testing device. Reading on the content of axiomatic design can found in Appendix J.

To make sure our device was working properly with the dynamometer, we designed the rope – pulley system that we eventually used as our final testing procedure. We found that the issues with how the testing device was attached to the dynamometer affected the data from the testing device. The testing device was designed to be directly fastened to the dynamometer, with parts touching above the force plate. This caused the testing device to apply a force on the dynamometer that caused issues with calibration. If the testing device was to be redesigned, it should be redesigned so that it does not apply a force on the dynamometer.

Figures 13 and 14 help illustrate the difference between the measurement with the testing device and the measurement with the rope – pulley system. Due to the forces the testing device was exerting on the dynamometer, the dynamometer only read a COF of 0.4 shown in figure 13, where we found a more realistic COF of 1.47 with the rope pulley system shown in figure 14. The dynamometer was able to accurately measure the forces simultaneously. If it was possible to account for the force the testing device had on the dynamometer, then we may have gotten similar results between the testing device and the rope-pulley system.

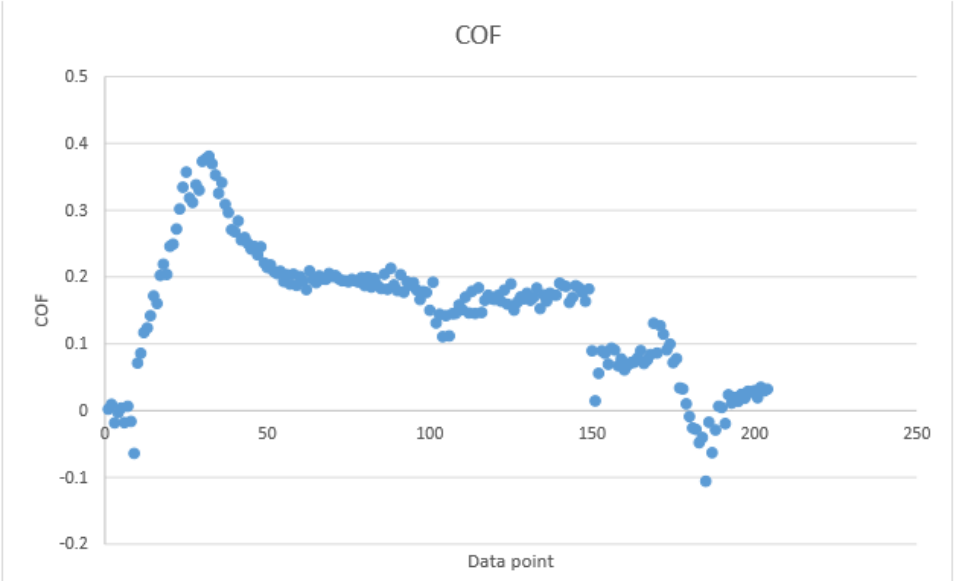

Figure 13: COF measurement using the testing device

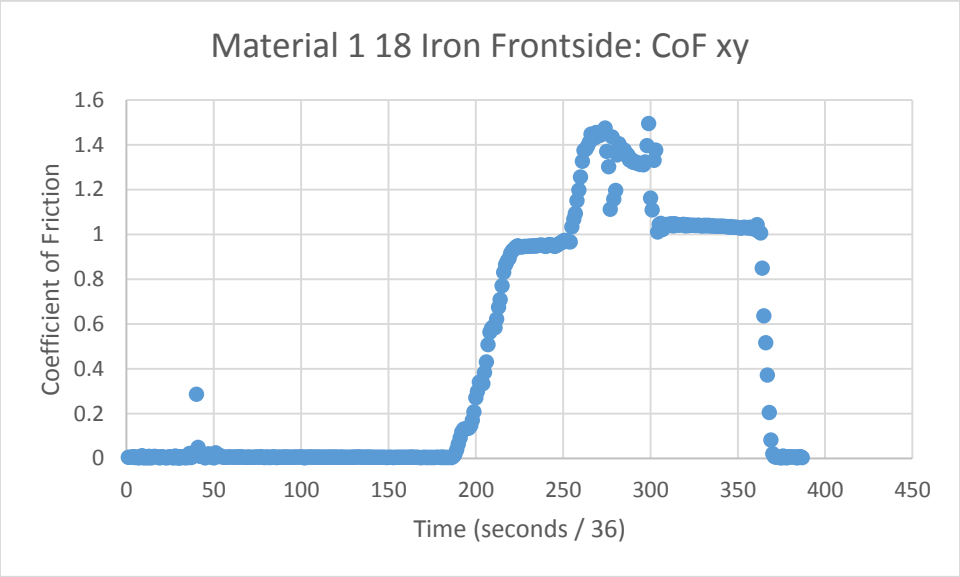

Figure 14: COF measurement using rope-pulley system

4.2 Surface Roughness

4.2.1 Discrimination Tests

When we analyzed the different surfaces of a material, we wanted to know if it was possible to distinguish between the surfaces at certain scales. To do this, our team used the program Sfrax to perform F-Tests on relative area of the surfaces in addition to area-scale complexity.

4.2.1.1 Relative Area

We performed f-tests at a 90% confidence level on the relative area of the surface measurements for both materials. If we wanted to repeat our measurements, we found that there were some comparison scales at a 90% confidence level at which we could repeat the same measurements. However, some of the mean square ratios did not seem to support our results. The confidence level indicated that the surfaces were only repeatable at the high scales. This result contradicts the results from the area – scale figure and regression analysis. Figure 15 shows one of the f-tests that demonstrates this finding for material one. The solid black line across the data points at a mean square ratio of approximately 3.21 indicates the crossover at which we would be able to be confident in repeating the same measurement. All data points above the black line are values we would feel confident in being able to repeat. In the figure, the line shows that the surfaces are distinguishable from 400 μm^2 and larger which does not support the findings of our relative area vs scale graph for material one found in the results. A full list of the discrimination tests for both materials can be found in Appendix H.

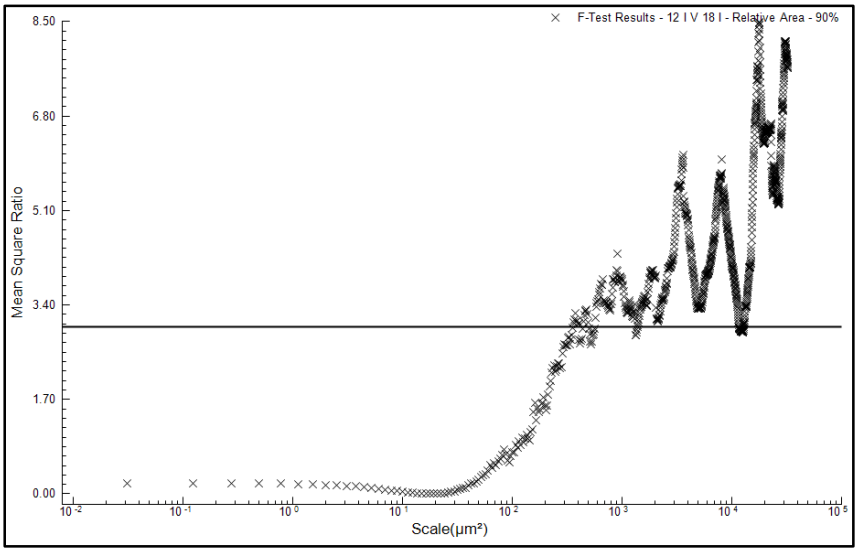

Figure 15: Discrimination Test between 12 iron mold and 18 iron mold

The discrimination tests are important for us to perform in order to confirm or deny that the results we receive from the regression analysis represent the four surface measurements we measured. The results we received from these tests are inconclusive and we are unable to say for all surfaces that we are 90% confident that we can distinguish between the four measurements.

4.2.1.2 Complexity

For the 90% confidence level f-tests on complexity of the surfaces, we found that the there were scales at which we could feel 90% confident that the measurements could be repeated. Figure 16 shows one of the figures that supports this finding for material one. The solid black line across the data points at a mean square ratio of approximately 3 indicates the crossover at which we would be 90% confident that the measurements could be repeated. In the figure, the line is around the 100 μm^2 scale which corresponds with the relative area vs scale graph for material one found in the results. A full list of the discrimination tests for both materials can be found in Appendix I.

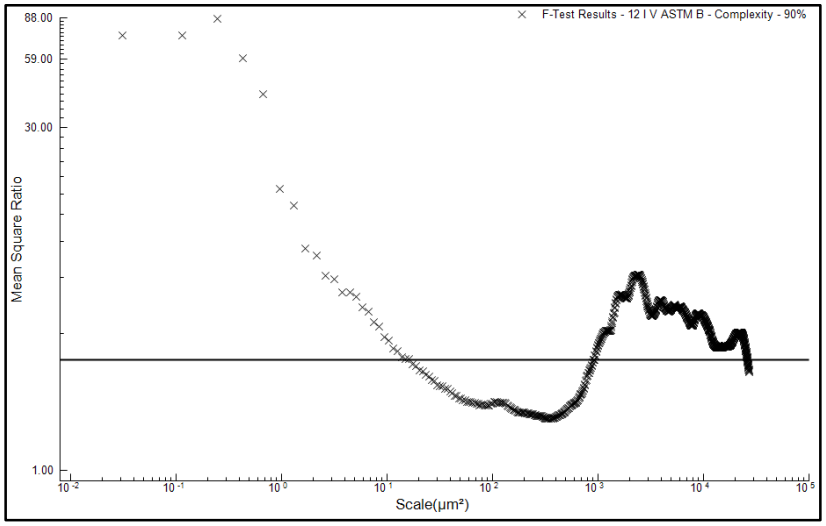

Figure 16: Discrimination test between 12 iron mold and ASTM mold

As with the relative area, the discrimination tests for complexity are important for us to perform in order to confirm that the results we receive from the regression analysis represent the four surface measurements we measured for each material. If we were unable to be confident that the measurements could be repeated for the four measurements, the results from the regression analysis would not be as conclusive.

4.2.2 Surfaces of Material

While our team was using the Olympus microscope, we found that the microscope could not measure two of the surfaces we intended to analyze. As seen in figures 17 and 18, two measurements taken at two different spots were showing nearly identical measurements. This happened for all six measurements on the same surface.

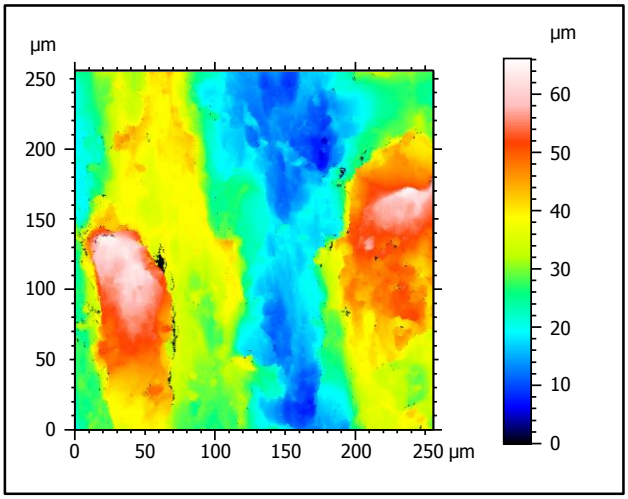

Figure 17: Surface Topography of Material 2 18 Iron Mold at Point A

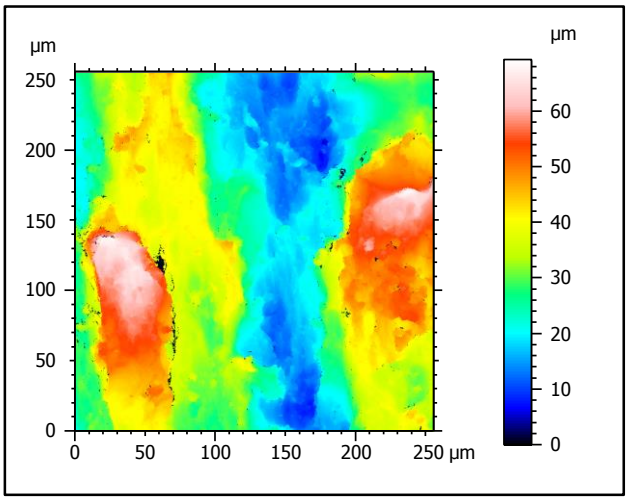

Figure 18: Surface Topography of Material 2 18 Iron Mold at Point B

We found that the issue with these surfaces was that Vibram buffed the materials by machines that are used for adhering the material to the midsole or outsole. This may have played a role in why the microscope could not measure the material, as this problem only existed with the buffed surfaces.

4.2.3.1. Counter Face Measurement

This project analyzed the surface roughness of the shoe sole material with COF measurements. The COF measurement is a measure of the forces interacting between the surface roughness of the shoe sole and the counter face. The surface roughness of the aluminum counter face used in our testing should have been analyzed, but unfortunately we ran out of time. Analyzing the surface of the counter face may provide further data to support the correlation between surface roughness and COF.

4.2.3. Surface Measurement Outliers

When performing our outlier removal procedure, we opted for the best method that would not alter the surface measurement. Several of the methods we analyzed in MountainsMap and SFrax removed the outlier completely from the measurement, leaving a non-measured point in the middle of the surface. Many of the methods attempted to fix this by an operator called fill in non-measured points. This operator takes the measurements surrounding the non-measured point and interpolates their measurements to produce a point that is most-likely what the measured point should be. However, the more outliers in a surface the more fill ins occur and alter the surface. Our team used the 85% slope filter in the remove outliers operator of MountainsMap because it removed the greatest outliers without leaving a large number of non-measured points.

Although our team was able to remove most of the outliers from the surface measurements, the 85% slope filter does not eliminate all outliers. Some outliers still existed in the measurement and could have had an effect on the correlation with COF. We recommend that a different outlier removal method be performed to eliminate all outliers without altering the surface measurement.

4.2.3.1. Height Parameters

In addition to the height parameters we measured, we tried to also measure the values for root mean square surface slope (Sdq) and developed interfacial area ratio (Sdr). However, due to the MountainsMap remove outliers operator, which affected the surface when we tried the fill in non-measured points option, we were unable to calculate these parameters due to the number of non-measured points in our measurement. If there is an option to remove outliers that do not create non-measured points, this would be ideal as the parameters Sdq and Sdr could be calculated and analyzed for correlation with COF.

4.2.4. Material Property Information

For this project, we wanted to test the surface roughness of shoe sole material to attempt to find data and a correlation relevant to shoe manufacturers. We teamed up with the Vibram Innovation Team in North Brookfield, MA to obtain material that was currently used to make shoes on the market. Unfortunately, due to the proprietary nature of the material, we were not able to receive full information on the material which could possibly be used to draw conclusions on correlation data.

4.3 Correlation

Due to time constraints, we were only able to measure two of the five materials provided to us by Vibram. Ideally, we would have been able to measure the surfaces of all five materials to have more correlation data. However, we feel that the two materials we measured still provide data that can be used to analyze the behavior of surface roughness as it relates to COF.

Additionally, due to the properties of the buffed surface, we were only able to analyze four surface measurements. Ideally, we would have been able to measure all six prepared surfaces for the

material. This would have enabled us to perform logarithmic regression analysis in addition to linear regression analysis. However, we feel that the surface measurements we received from the microscope were able to provide us with data needed to make conclusions about the correlation between surface roughness and COF.

5. Conclusions

1. Surface relative area and complexity do have a correlation with COF measurements with an R^2 value at 0.99 for material one at a scale of 100 μm^2 and smaller.
2. Surface relative area does have a correlation with COF measurements with an R^2 value at 0.47 for material two at a scale of 100 μm^2 and smaller.
3. Complexity does have a correlation with COF measurements with an R^2 value at .84 for material two at a scale of 8 μm^2 and smaller.
4. Our results indicate that a material with a modulus of elasticity of 7.042×10^6 has a higher R^2 value than a material with a modulus of elasticity of 4.899×10^6 when correlating relative area with COF.
5. For relative area and complexity, there are mean square ratios for some surfaces that can provide a 90% confidence level that our measurements can be repeated at small scales.
6. Conventional surface height parameter Sp does have a correlation with COF measurements with an R^2 value at 0.8184 for material two.
7. Conventional surface volume parameters Vmp, Vmc, and Vvc do have a correlation with COF measurements at an R^2 value above 0.8 for material one.

References

Ahn, D., Kweon, J., Choi, J., & Lee, S. (2011). Quantification of surface roughness of parts processed by laminated object manufacturing. Journal of Materials Processing Technology, 212(2), 339. doi:10.1016/j.jmatprotec.2011.08.013

Brown, R. (1999). Handbook of polymer testing: Physical methods Taylor & Francis.

Chang, W., & Matz, S. (2001). The slip resistance of common footwear materials measured with two slipmeters. Applied Ergonomics, 32(6), 549-558. doi:10.1016/S0003-6870(01)00031-X

Chen, Z., Lu, X., Chan, C. -., & Mi, Y. (2006). Manipulating the surface properties of polyacrylamide with nitrogen plasma. European Polymer Journal, 42(11), 2914-2920. doi:10.1016/j.eurpolymj.2006.08.007

Clarke, J. D., Hallas, K., Lewis, R., Thorpe, S., Hunwin, G., & Carré, M. J. (2015). Understanding the friction measured by standardised test methodologies used to assess shoe-surface slip risk. Journal of Testing and Evaluation, 43(4), 1-12. doi:10.1520/JTE20120334

Deltombe, R., Kubiak, K. J., & Bigerelle, M. (2014). How to select the most relevant 3D roughness parameters of a surface. Scanning, 36(1), 150-160. doi:10.1002/sca.21113

Derler, S., Kausch, F., & Huber, R. (2008). Analysis of factors influencing the friction coefficients of shoe sole materials. Safety Science, 46(5), 822-832. doi:10.1016/j.ssci.2007.01.010

Derler, S., Kausch, F., & Huber, R. (2008). Analysis of factors influencing the friction coefficients of shoe sole materials. Safety Science, 46(5), 822-832. doi:10.1016/j.ssci.2007.01.010

Fendley, A., Marpet, M. I., & Medoff, H. (1995). The friction-related component of a comprehensive slip-prediction model. II. use of ratiometric analysis and thresholded dimensionless numbers. Proceedings of the 1995 Fourteenth Southern Biomedical Engineering Conference, , 162-165. doi:10.1109/SBEC.1995.514467

Hu, K., Jiang, X., Liu, X., & Xu, Z. (2006). Comparison between ASME and ISO standards on surface texture. Proceedings of SPIE, 6280(1) doi:10.1117/12.716169

Kiu, K. Y., Stappenbelt, B., & Thiagarajan, K. P. (2011). Effects of uniform surface roughness on vortex-induced vibration of towed vertical cylinders. Journal of Sound and Vibration, 330(20), 4753-4763. doi:10.1016/j.jsv.2011.05.009

Kistler Group. (2015). *Instruction Manual: Quartz 3-Component Dynymometer Type 9257B*. Switzerland: Kistler Group.

Li, K. W., Chang, W. R., Wei, J., & Kou, C. (2006). Friction measurements on ramps using the brungraber mark II slipmeter. Safety Science, 44(5), 375-386. doi:10.1016/j.ssci.2005.11.003

Li, K. W., Chang, W., Leamon, T. B., & Chen, C. J. (2004). Floor slipperiness measurement: Friction coefficient, roughness of floors, and subjective perception under spillage conditions. Safety Science, 42(6), 547-565. doi:10.1016/j.ssci.2003.08.006

Li, K. W., Wu, H. H., & Lin, Y. (2006). The effect of shoe sole tread groove depth on the friction coefficient with different tread groove widths, floors and contaminants. Applied Ergonomics, 37(6), 743-748. doi:10.1016/j.apergo.2005.11.007

Prodanov, N., Gachot, C., Rosenkranz, A., Mücklich, F., & Müser, M. H. (2013). Contact mechanics of laser-textured surfaces: Correlating contact area and friction. Tribology Letters, 50(1), 41-48. doi:10.1007/s11249-012-0064-z

Snedecor, George W. and Cochran, William G. (1989), Statistical Methods, Eighth Edition, Iowa State University Press.

Zhou, B., Wang, X., Gho, W. M., & Tan, S. K. (2015). Force and flow characteristics of a circular cylinder with uniform surface roughness at subcritical reynolds numbers. Applied Ocean Research, 49, 20-26. doi:10.1016/j.apor.2014.06.002

Appendix

Appendix A

We were provided information on the polymer samples, but due to their proprietary nature we are unsure of the complete composition of the material. Table 1 and Table 2 show the information available for all five materials we received.

	Base Polymer	Tensile (psi)	Elongation (%)
1	Butyl Base Polymer	2639	882
2	NBR / PVC	1724	670
3	SBR, IR	2625	560
4	CR	2590	535
5	NBR	1938	649

Table 6: Tensile Strength and Elongation Percentage for the 5 Polymer Samples

	Base Polymer	Strain at Break (mm/mm)	Stress at Break (MPa)	Modulus of Elasticity (Pa)	Tg (C)
1	Butyl Base Polymer	3.09+- 0.19	21.76+-0.85	7.042×10^6	-35C
2	NBR / PVC	2.18+-0.20	10.68+-0.81	4.899×10^6	-15C

Table 7: Strain, Stress, Modulus of Elasticity, and Glass Transition Temperature for Samples 1 and 2

Vibram also provided us with information on how they molded and buffed the material. This information is listed below.

Molding:

- We run a compression molding operation
- Our factory in the US has over 40 presses running to make soles
- Compression presses cure the rubber using a combination of heat and a large amount of pressure
- The presses run at around 350F and the time they run at depends on the thickness and shape of the individual soles
    - Some of the presses in the factory can run up to 500F though our material doesn't normally need that much heat
    - Soles take approx. 10 min in the cure / molding process – as a baseline
- The molds inside the presses are made of steel and are different sizes depending on the sole as well

Buffing:

- For buffing we have a few different types of machines
    - Some of the machines are made to buff the rubber outsoles – this helps the shoe company adhere them to the midsole
    - Other machines are made to buff the midsole for the same reasons

    - We also make sheets of material in the factory – those are buffed by much larger machines that buff one side at a time
- Mostly buffing is done for adhesion purposes

Appendix B

We designed the spacer in SolidWorks and manufactured using a 3D printer. The dimensions of the block are 1.75” X 1.75” X 0.5”. We designed this spacer to allow us to apply the necessary normal force and tangential force using various weights. The rubber material was adhered to the spacer through the use of an epoxy glue, Loctite Flexible Adhesive for vinyl, fabric, plastic and also rubber, which needed 24 hours to set. Figure 19 shows the 3D printed block with the rubber material adhered to it.

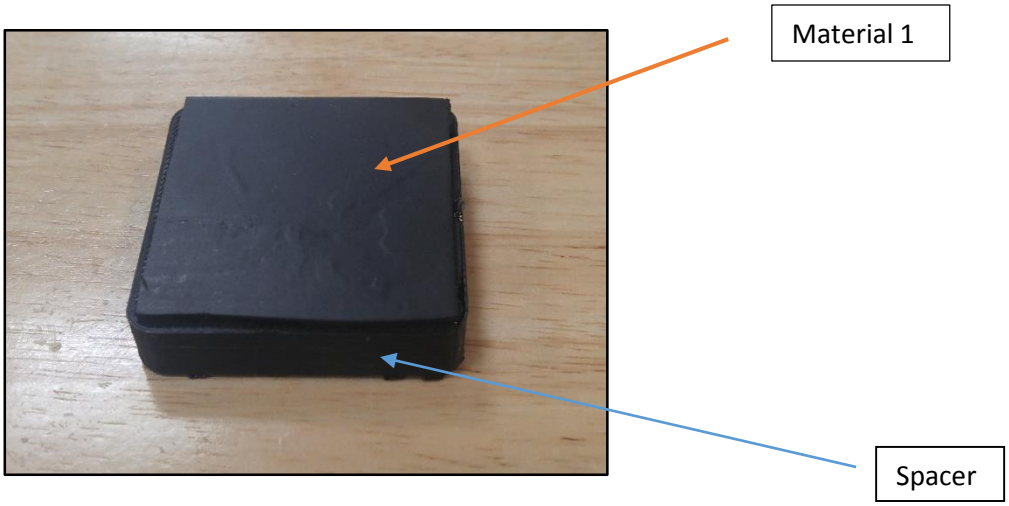

Figure 19: Rubber Material Adhered to Spacer

Appendix C

“The multicomponent dynamometer provides dynamic and quasi-static measurement of the 3 orthogonal components of a force (Fx, Fy, and Fz) acting from any direction onto the top plate” (Kistler Group 2015). The dynamometer allowed this project to measure the normal and tangential forces simultaneously. We were then able to calculate the COF that could be used to attempt to correlate COF with surface roughness parameters.

The dynamometer requires a signal amplifier. This amplifier takes the change in electrical charge from the dynamometer, amplifies it by a desired voltage per mechanical unit, and reports the forces in the form of three voltages, one for each orthogonal direction. To read these three analog signals we used a National Instruments DAQ box. The DAQ box was connected to a computer running a virtual instrument (VI) which can read all three of these signals simultaneously. The VI, programed through LabView, has the capability to be calibrated to any unit of force.

Appendix D

Measuring the forces of friction involved calibrating the dynamometer. We needed to use the voltages that the dynamometer and LabView produce and convert them into a unit of weight. To do this, we placed known weights on top of the dynamometer. This process involved placing a 2.5lb weight on

the dynamometer and recording the weight the dynamometer was measuring. We repeated this process for 5lb, 7.5lb, 10lb, and 12.5lb weights. The LabView program recorded the measurements and exported the data to an Excel sheet. The recorded values were plotted against the actual weight values and a linear regression analysis was performed. The intercept of the equation found through the analysis was used as the offset value when recording COF data through Labview. This calibrated the dynamometer by offsetting the difference in measurement between the known weight and the weight measured by the dynamometer. Figures 20 and 21 show how we calibrated in the normal and tangential directions.

For calibrating the tangential direction, we created a rope - pulley system. For all measurements, we used an aluminum plate as our common counterface for finding the COF. To attach the aluminum plate to the dynamometer, we screwed the aluminum piece into the threaded hole of the Kistler dynamometer closest to the pulley at the edge of the table. We attached the rope to the head of the threaded rod and attached different weighted plates to the end of the rope hanging from the pulley. We followed the same procedure from the calibration of the normal force in placing weights and recording the measurements to find the offset value for tangential force. Figure 21 shows how we calibrated the force in the tangential direction. Figure 22 shows how we interpreted the data in Excel to get the offset value used during the measurement procedure.

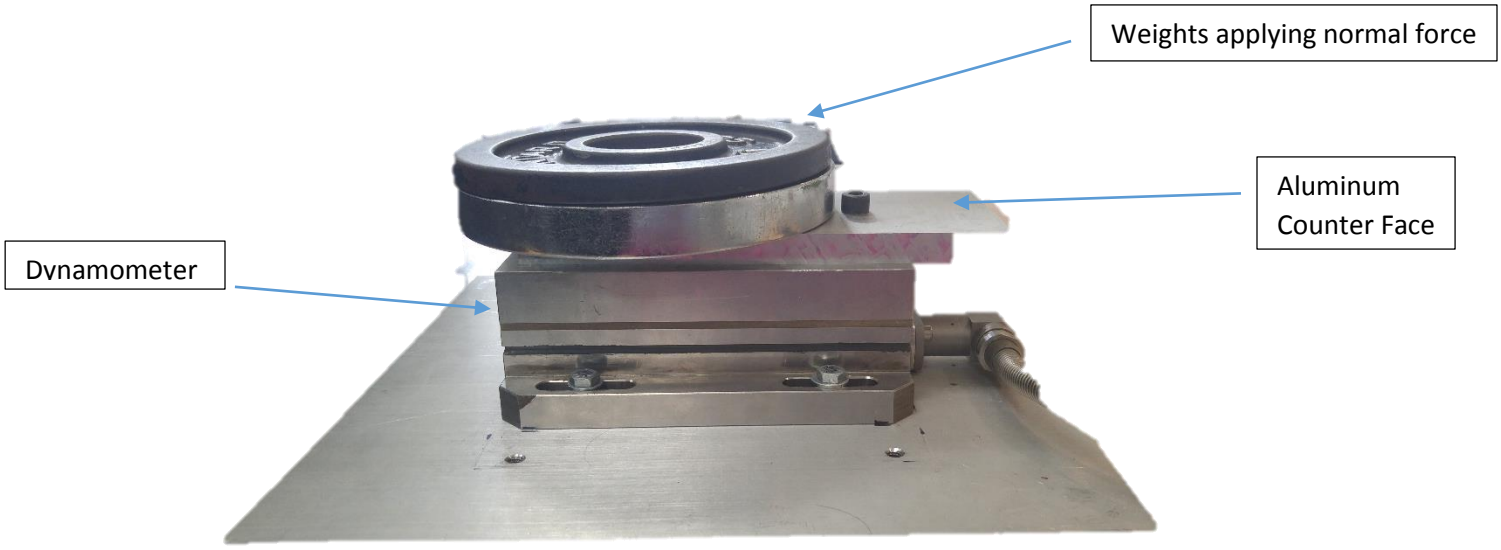

Figure 20: Normal Force Calibration

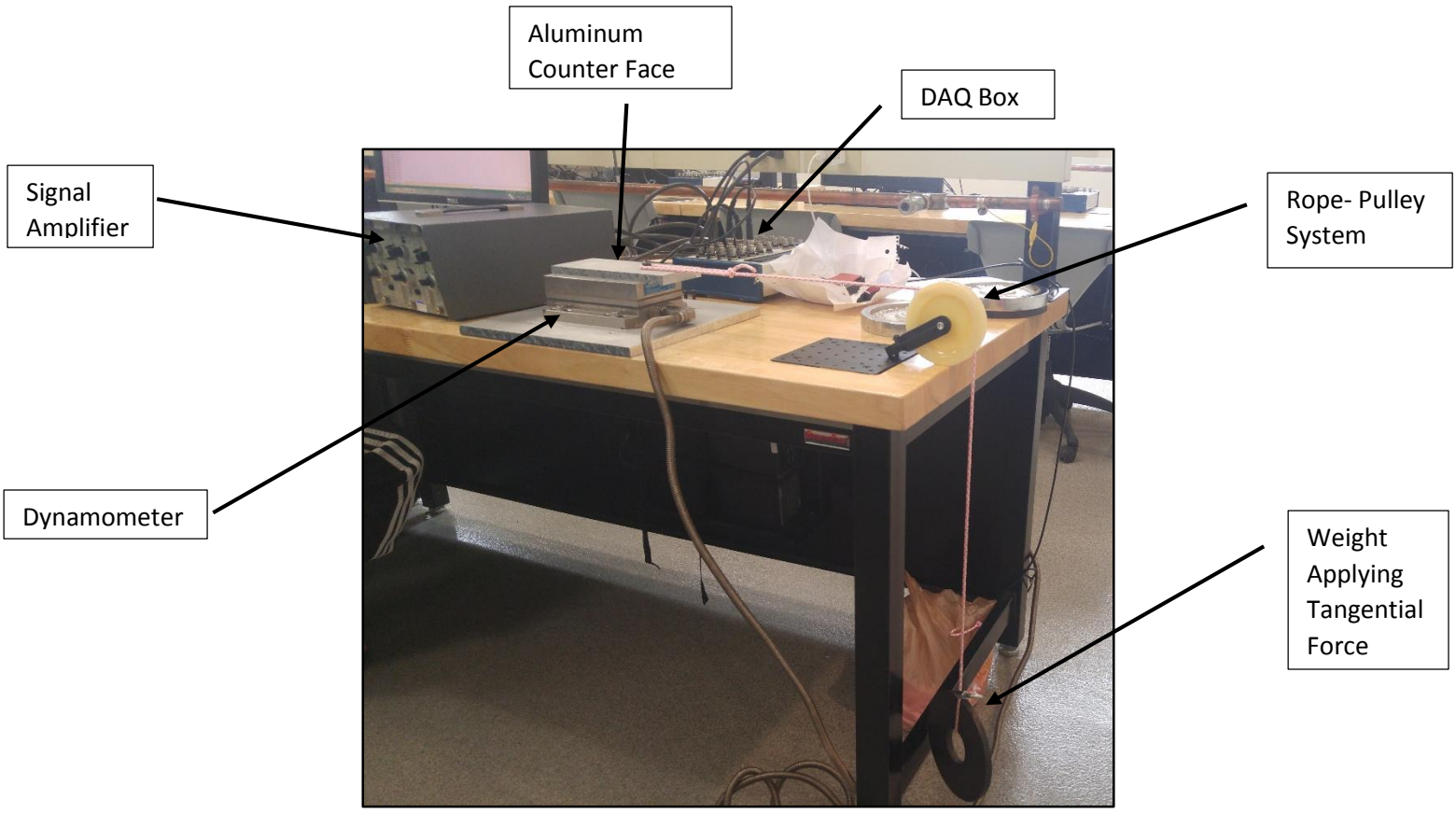

Figure 21: Tangential Force Calibration

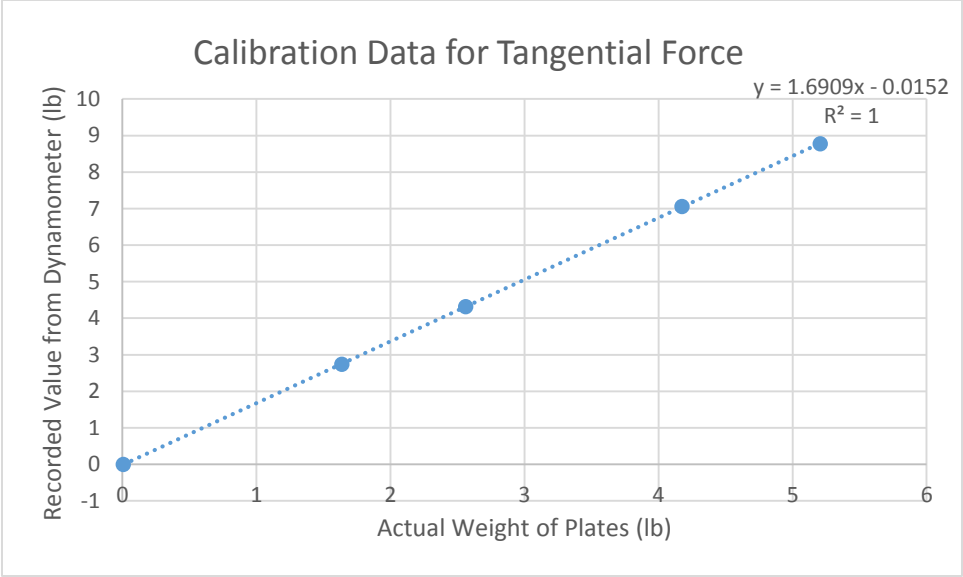

Figure 22: Calibration Data for Tangential Force

Appendix E

To apply a normal force, a weight was placed on the spacer. The side of the spacer with the surface adhered to it was placed on the aluminum counterface. We secured the aluminum piece with a bolt into the threaded hole the Kistler dynamometer closest to the pulley at the edge of the table. The aluminum counterface acted as the common counterface among all of the testing trials. To apply a tangential force, we attached the small rope – pulley system used in the set-up around the edges of the spacer underneath the weight and above the rubber material. We attached a weight to the end of the

rope and slowly lowered it down until it hung from the pulley system at the edge of the table. If the weight did not move the material across the counterface, we applied a small additional force on the rope until the material slid. The material slipping over the counterfaace indicated that we reached the static COF limit which would be represented in the data set as the highest point of force. We designed a LabView program that could export the data from the measurement to an Excel worksheet where we could interpret the measurements. We repeated this process six times so that we could calculate the average COF for each surface. Figure 23 shows how we set up the COF measurement.

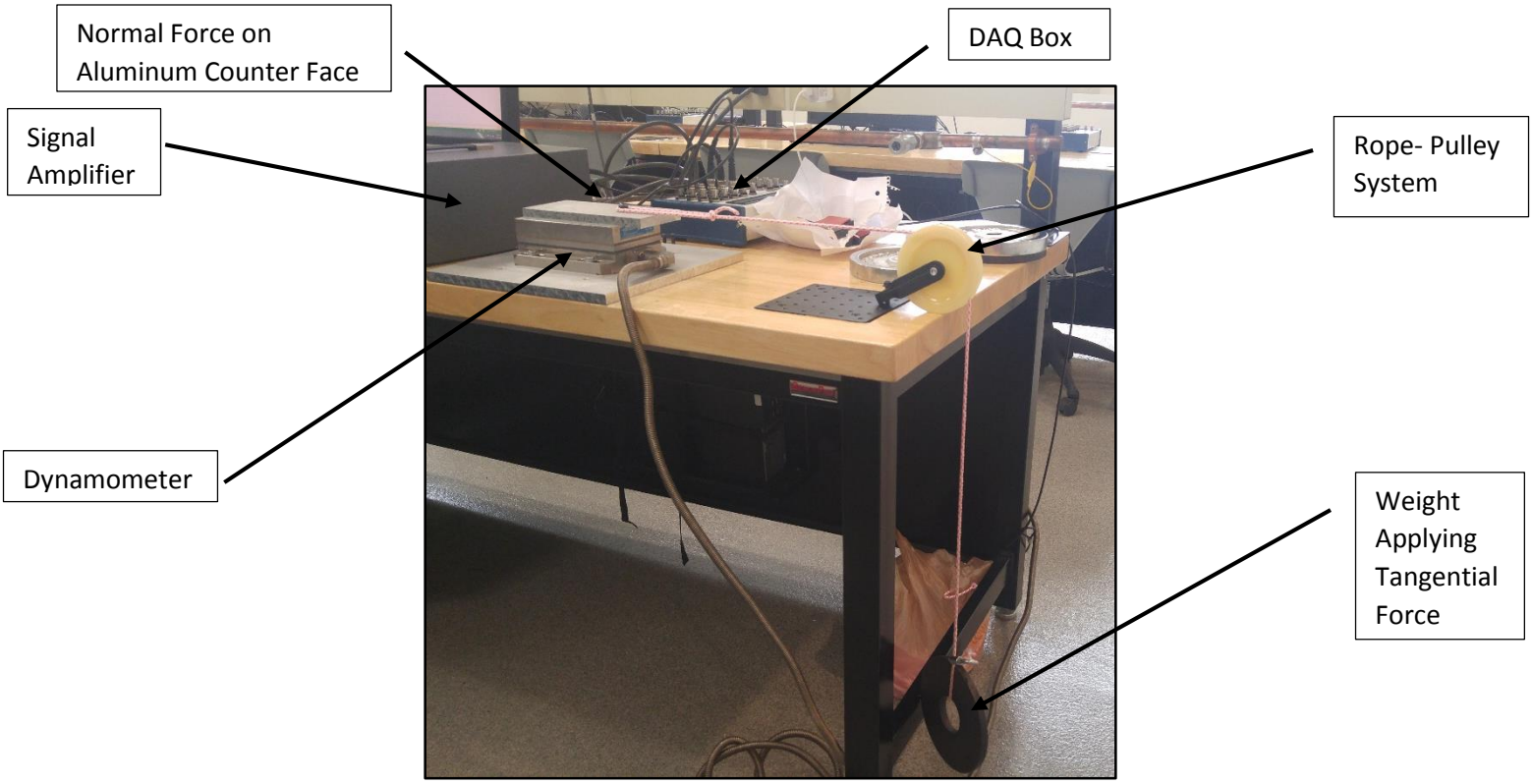

Figure 23: Friction Measurement

Appendix F

To prepare the material for measurement, the team cleaned the surface with soap and water. We dried the material with Dust Off compressed air in an attempt to eliminate contamination in the measurement. The material was prepared in samples of 1.75” x 1.75” and measured with the x50APO lens. This lense measures at a field of view of 256-32 µm. As the image size taken by the microscope is in nanometers and the materials surface 1.75 inches x 1.75 inches, we measured six different points on the same surface. Our team was then able to calculate the average surface roughness parameters in order to analyze the correlation between surface roughness and COF.

Appendix G

Because we took six different measurements on the same surface, our team needed to stitch the measurements together to get an average value for the surface roughness properties.

MountainsMap Remove Outliers Operator

While taking a measurement, the Olympus microscope takes measurements of the surface that are considered outliers, or not true representations of the surface. These outliers can affect the surface roughness parameters and need to be removed. The MountainsMap operator for removing outliers removed any outliers outside of 85% of the slope of the surface. The program analyzed and determined the height and slopes all of the peaks of the surface measurement. To remove outliers, the user can choose how much of the surface they want removed. In this instance, we chose to remove any points that had a slope greater than 85% of the average slope of the surface. Additionally, the program requires removing points as strong, normal, or soft. We chose the soft removal because it removed points that the strong and normal methods did not. Figure 24 shows the instruction panel for removing outliers that we used. Figures 25 and 26 show the original surface and the surface with the outliers removed. Figure 25 and Figure 26 illustrate how the operator removed the outliers.

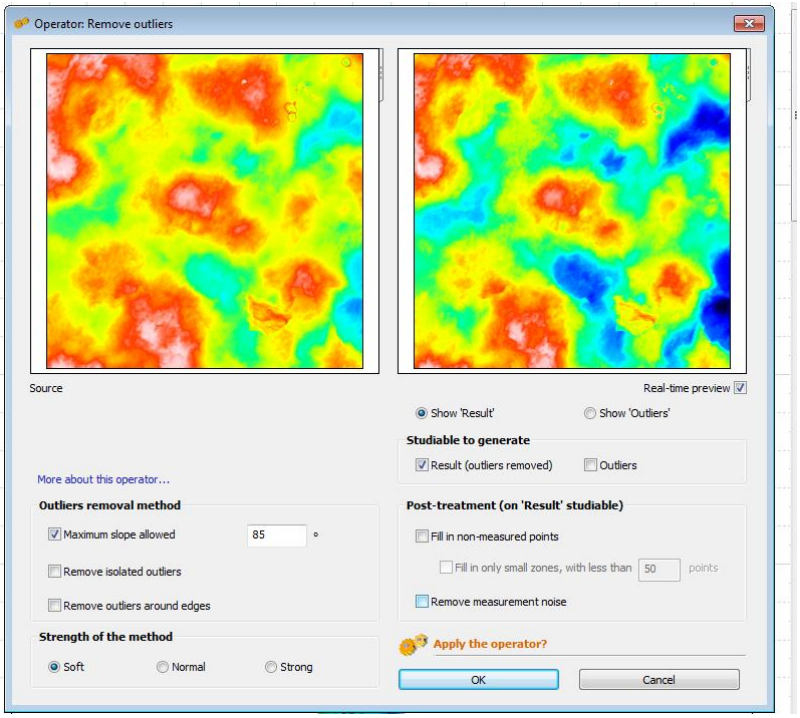

Figure 24: Instruction panel for MountainsMap remove outliers operator

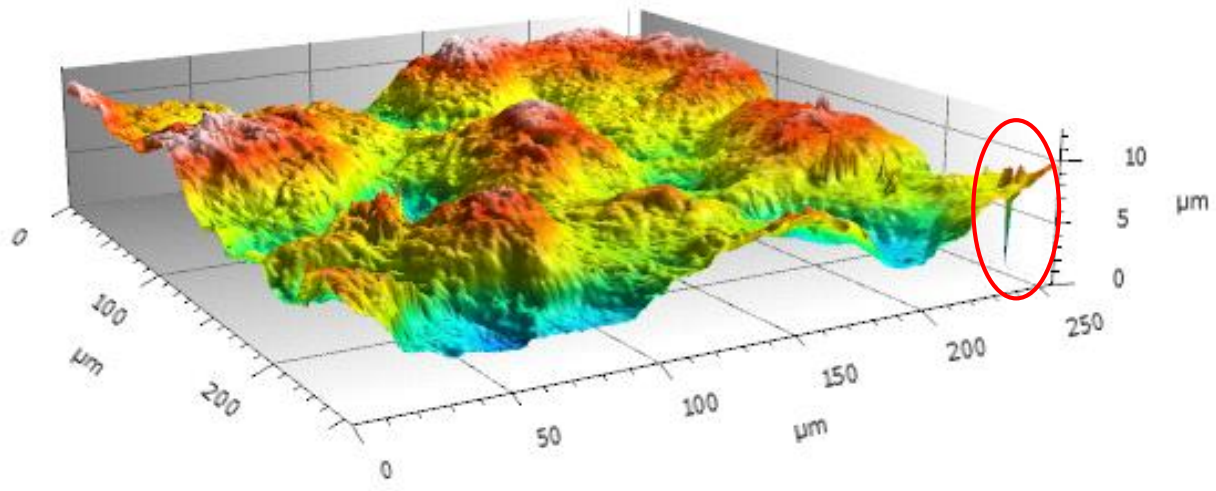

Figure 25: Material 2 surface topography with outliers

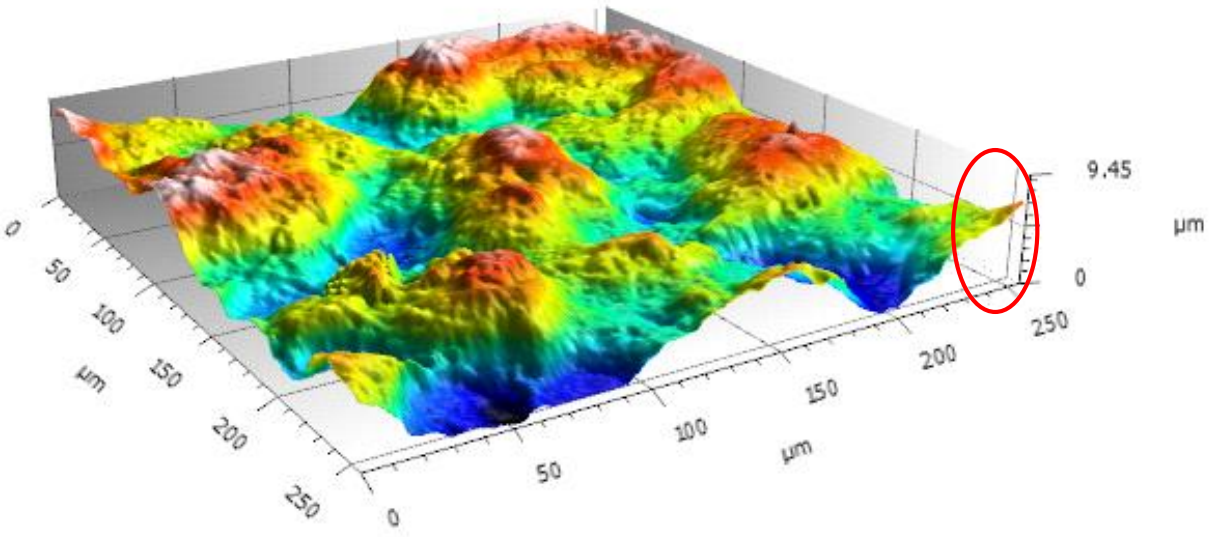

Figure 26: Material 2 surface topography with outliers removed

MountainsMap Level Operator

A surface can be unbalanced when taking a measurement with the microscope at these fine scales. Leveling the surface measurement is important to ensure that an unbalanced measurement will not affect the surface roughness parameters. This function has several different selections for leveling a surface. Through testing each method we were able to find a function that leveled surface without changing the surface measurement. We chose to level through the least squares plane method. This method analyzes a surface and fits the points to a best fit line curve. Additionally this method was performed by the operation subtraction compared to the line by line operation. We chose to use subtraction over line by line to produce a leveled surface that did not change the surface measurement.

Figure 27 shows the instruction panel for leveling the surface that we used. Figure 28 shows one of surfaces after applying the level operator.

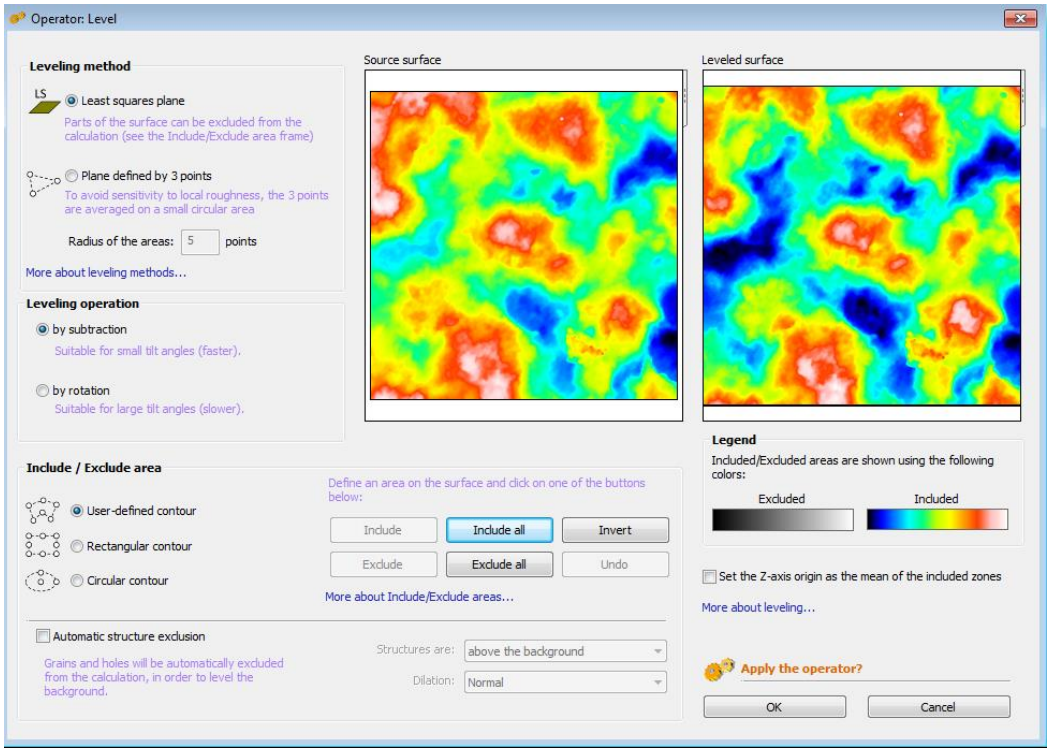

Figure 27: Instruction panel for MountainsMap level operator

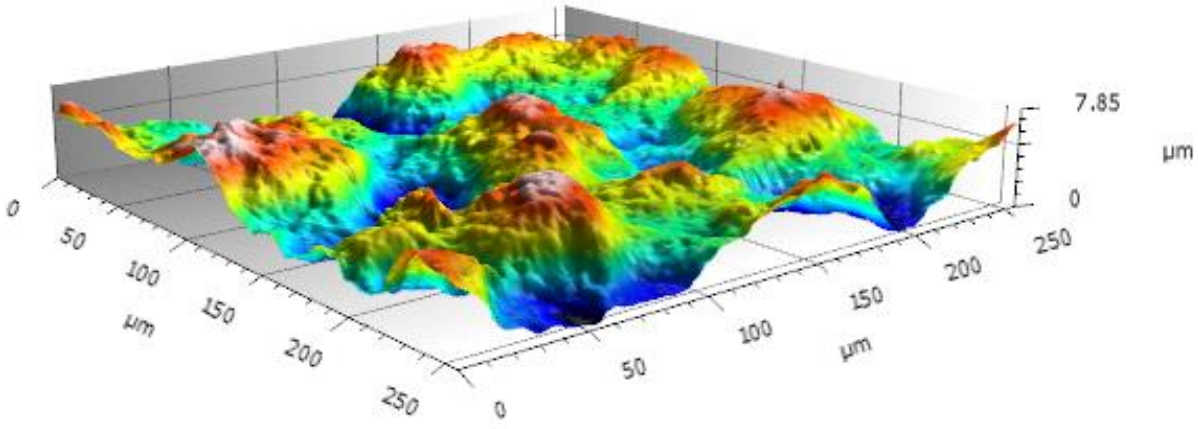

Figure 28: Leveled surface

MountainsMap Stitch Operator

We used MountainsMap in order to stitch the six measurements together, remove the outliers from the measurements, and level any unbalanced measurements. This eliminates any factor that could influence the analysis of the correlation between COF and surface roughness. For stitching, we used the stitch method in MountainsMap to combine our six measurements on the same surface together. This

would provide us with a single surface measurement, averaging the measurements of all six measurements. The operator allows the user to choose a grid on which to place each surface measurement for stitching. As we chose to take three measurements on the top half of the surface and three measurements on the bottom half of the surface, we chose a 3 X 2 grid to stitch the measurements together. Figure 29 shows the instruction panel for stitching the surface measurements together. Figure 30 shows one of the surfaces after applying the stitch operator.

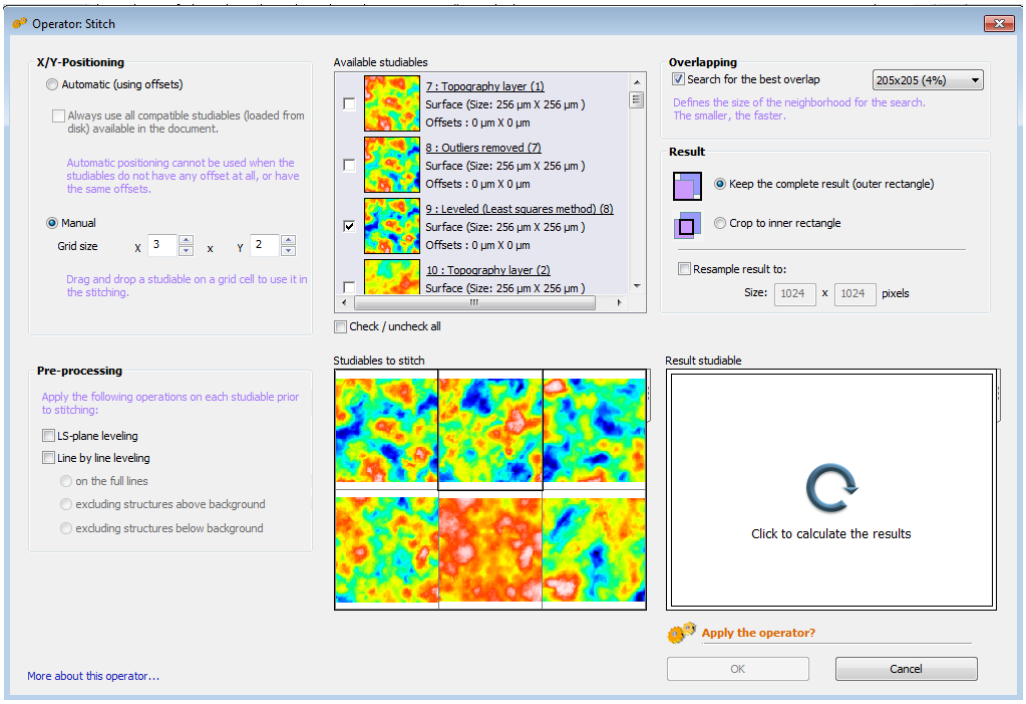

Figure 29: MountainsMap Instruction Panel or stitching surfaces

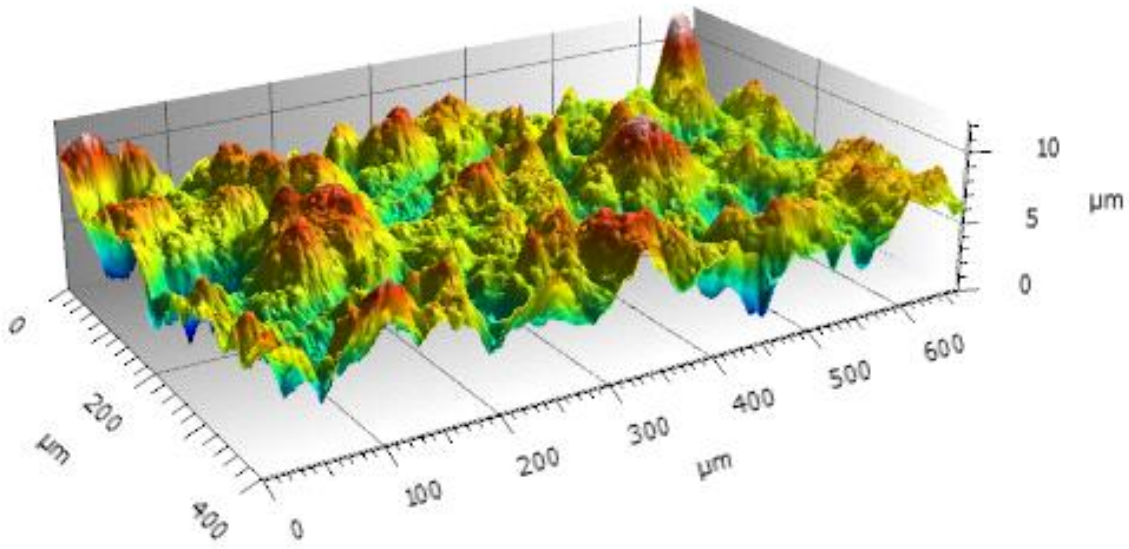

Figure 30: Stitched Surfaces in MountainsMap

Appendix H:

Relative Area Discrimination Analysis

90% Confidence Interval F-Test for Material 1

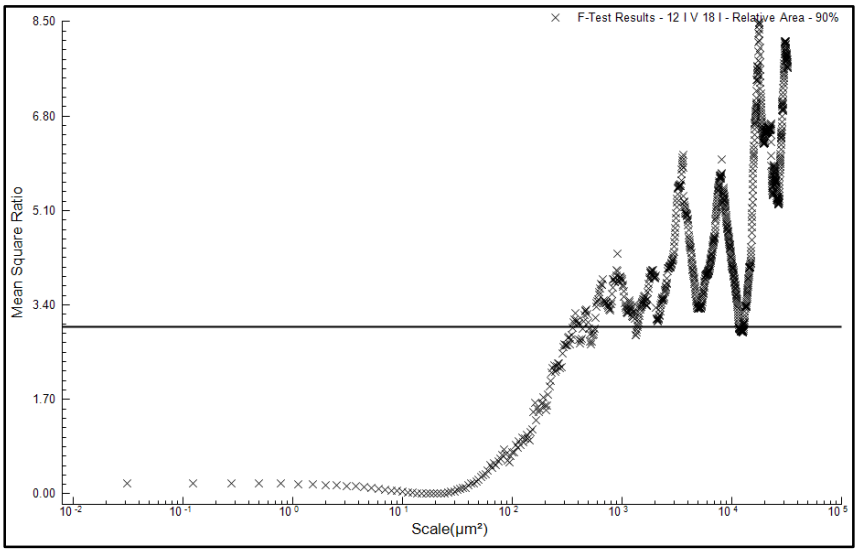

Figure 31: 12 Iron Surface against 18 Iron Surface

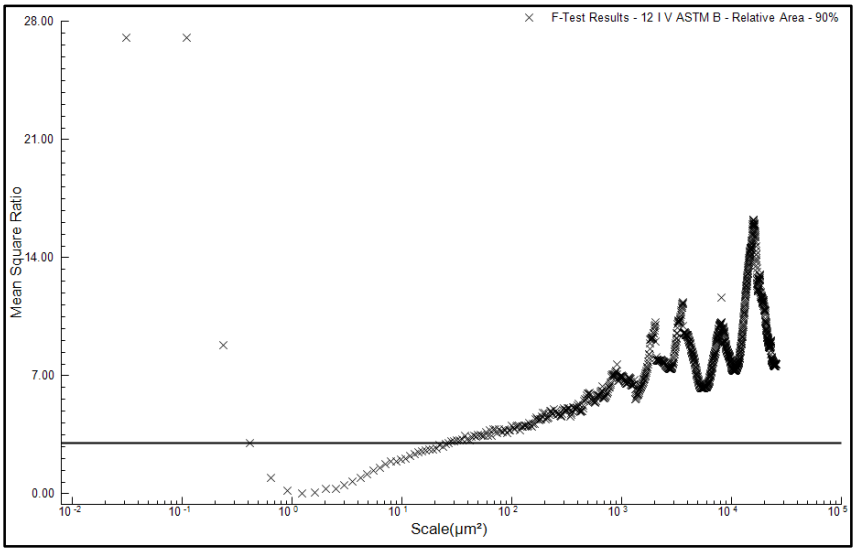

Figure 32: 12 Iron Surface against ASTM Back Side Surface

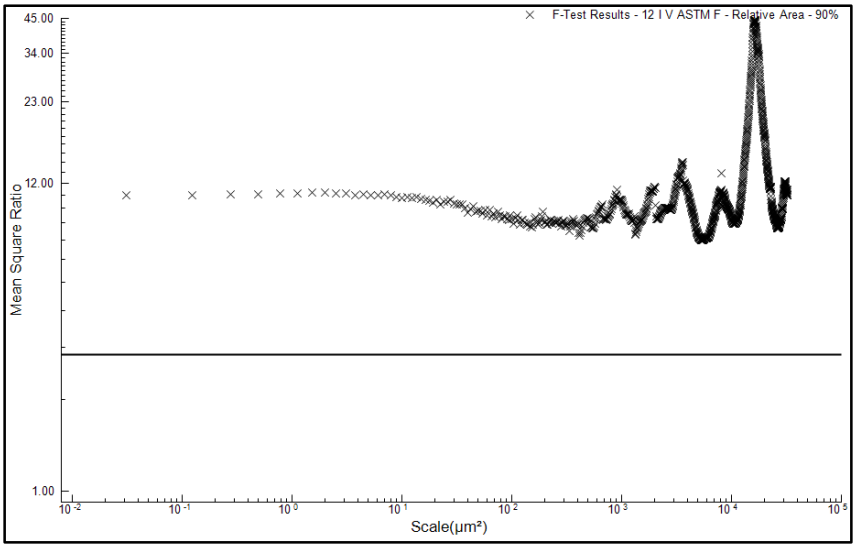

Figure 33: 12 Iron Surface against ASTM Front Side Surface

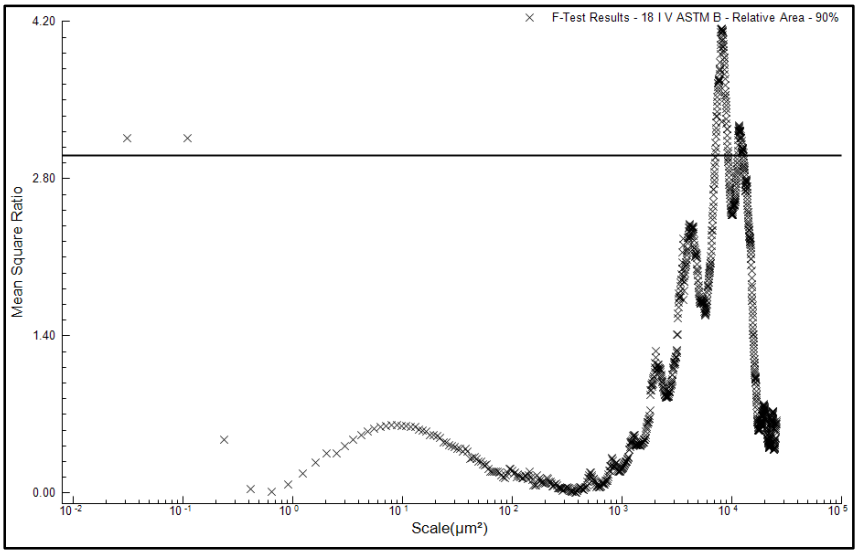

Figure 34: 18 Iron Surface against ASTM Back Side Surface

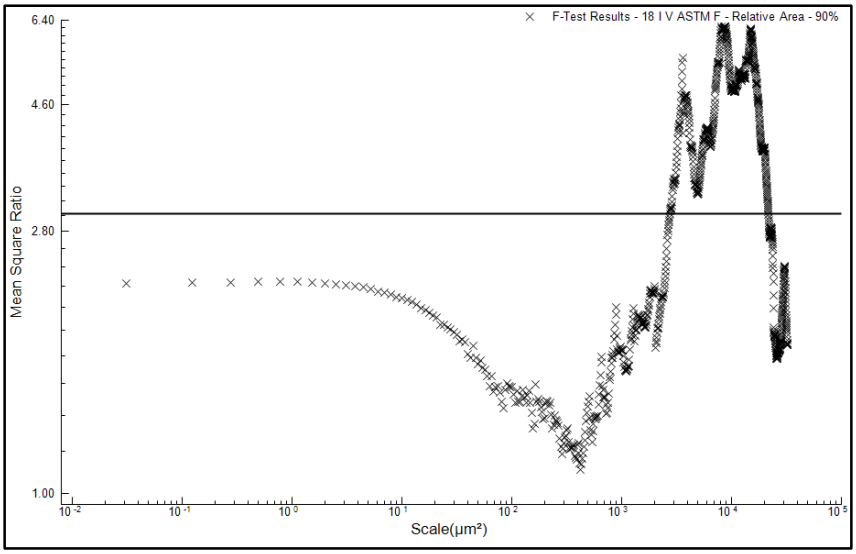

Figure 35: 18 Iron Surface against ASTM Front Side Surface

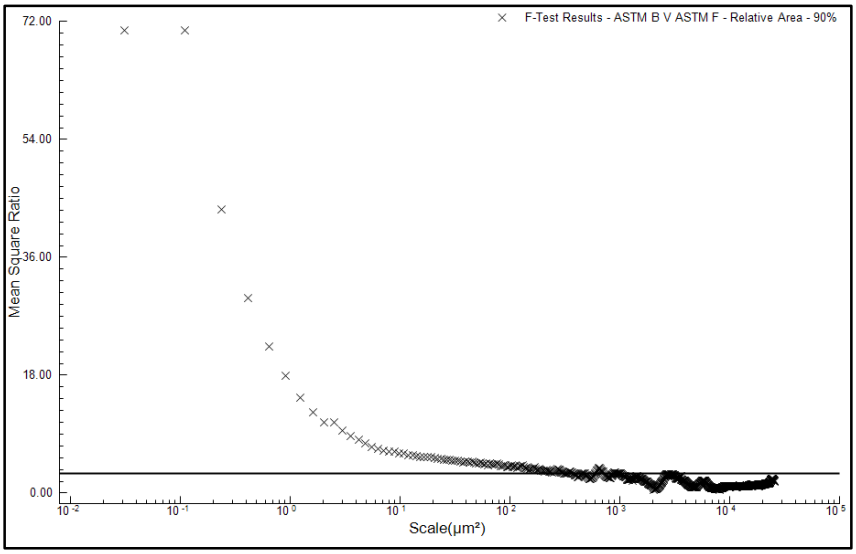

Figure 36: ASTM Back Side Surface against ASTM Front Side Surface

90% Confidence Interval F-Test for Material 2

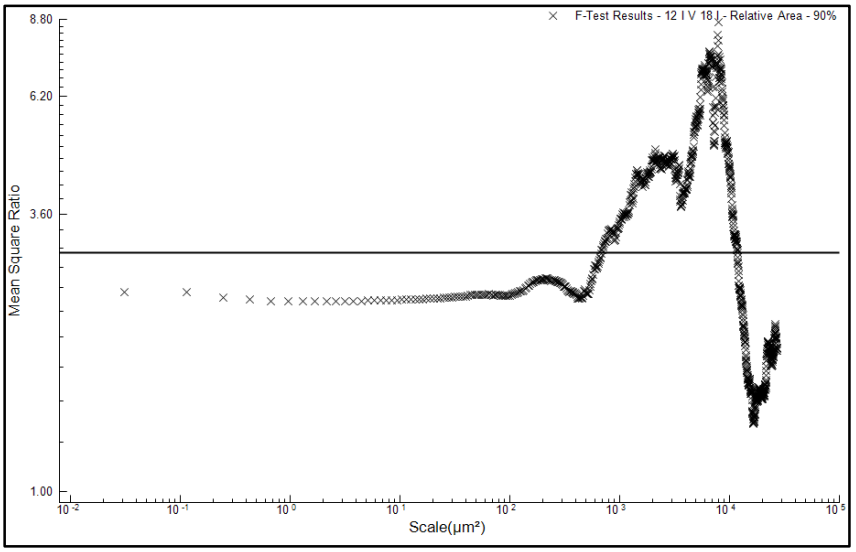

Figure 37: 12 Iron Surface against 18 Iron Surface

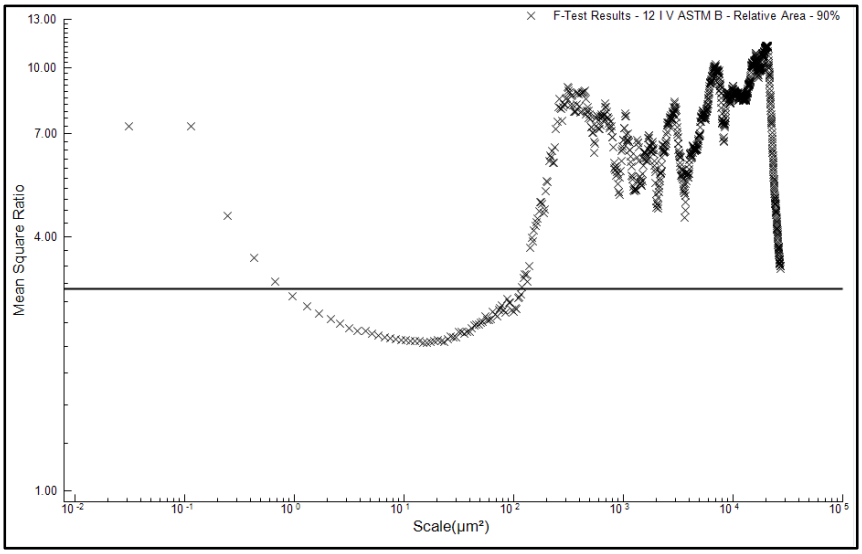

Figure 38: 12 Iron Surface aginast ASTM Back Side Surface

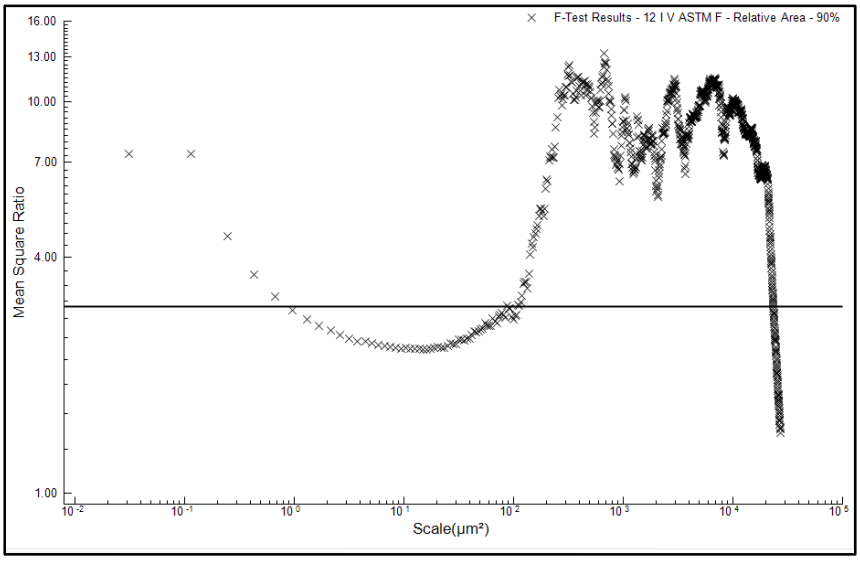

Figure 39: 12 Iron Surface against ASTM Front Side Surface

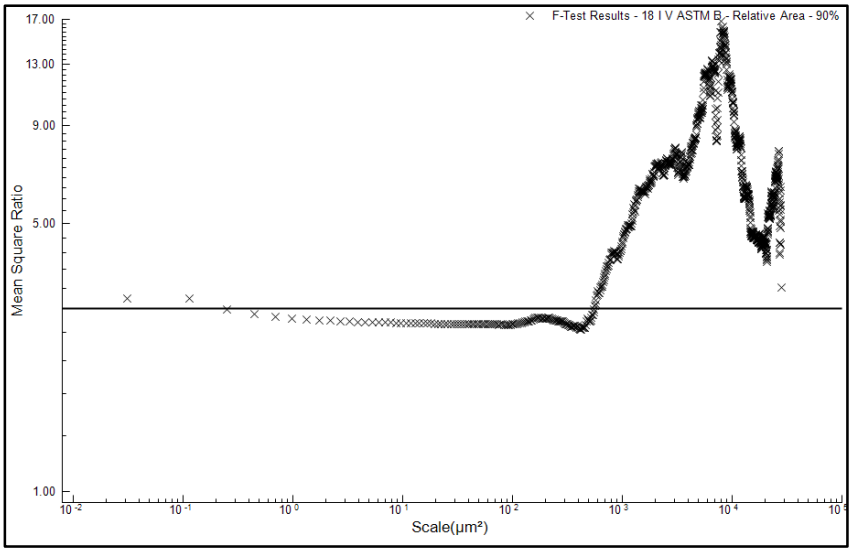

Figure 40: 18 Iron Surface against ASTM Back Side Surface

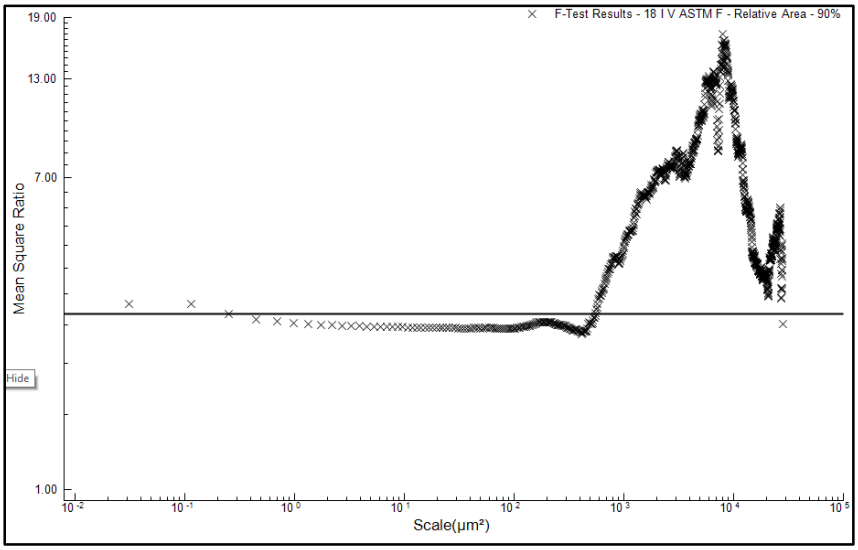

Figure 41: 18 Iron Surface against ASTM Front Side Surface

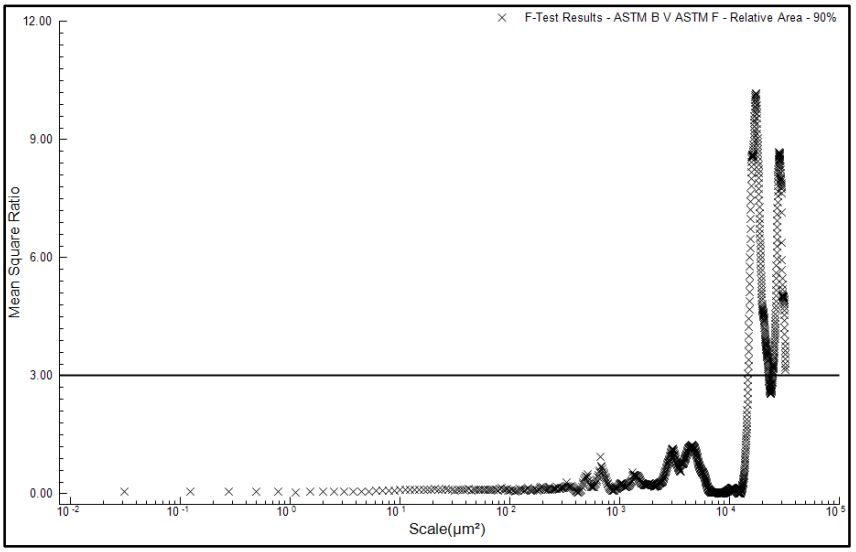

Figure 42: ASTM Back Side Surface against ASTM Front Side Surface

Appendix I:

Complexity-Scale Discrimination Analysis

90% Confidence Interval F-Test for Material 1

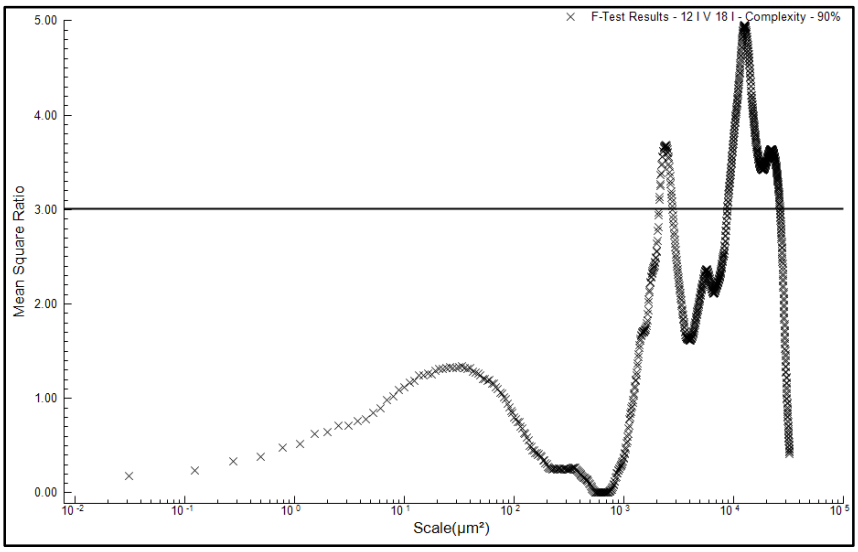

Figure 43: 12 Iron Surface against 18 Iron Surface

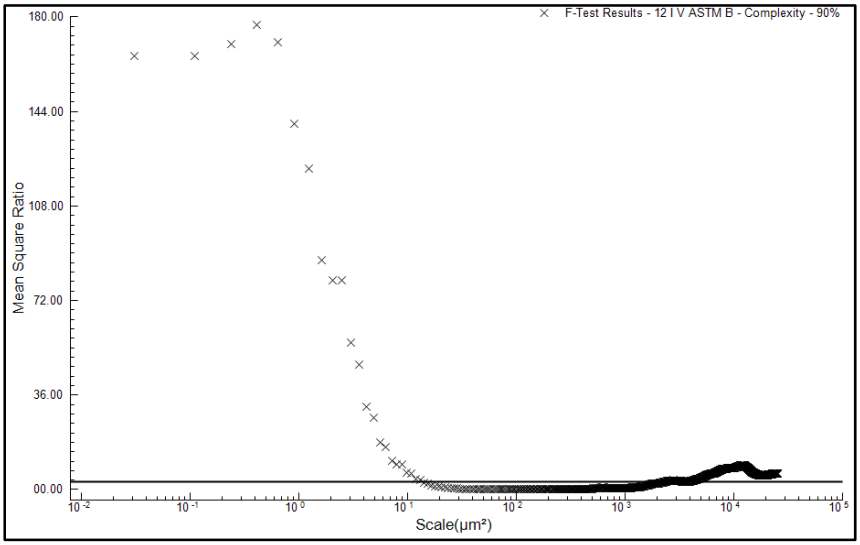

Figure 44: 12 Iron Surface against ASTM Back Side Surface

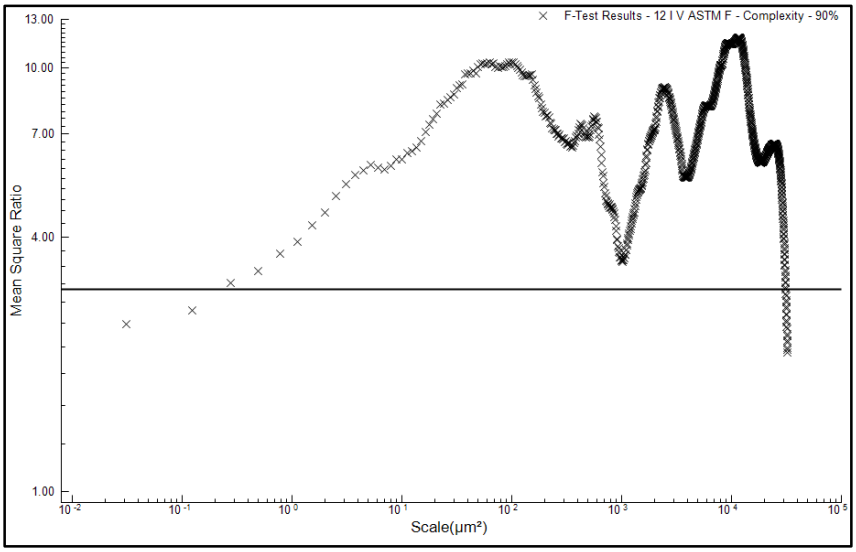

Figure 45: 12 Iron Surface against ASTM Front Side Surface

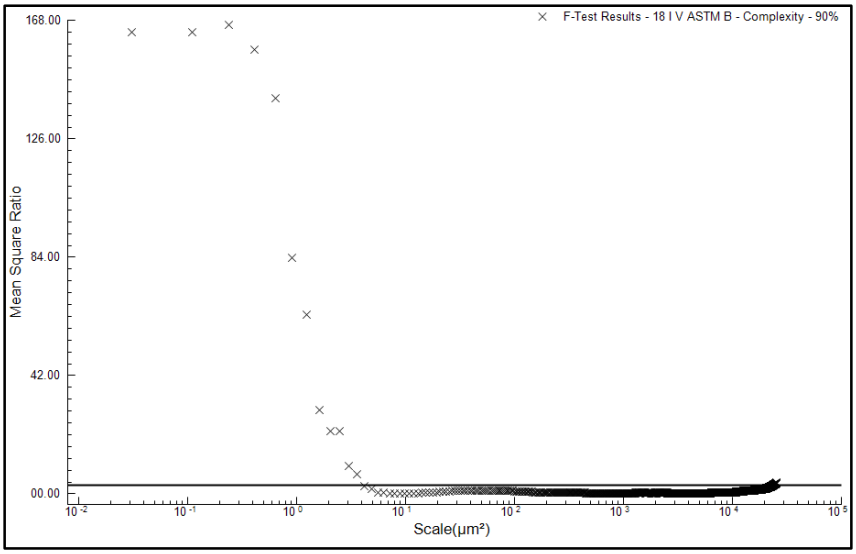

Figure 46: 18 Iron Surface against ASTM Back Side Surface

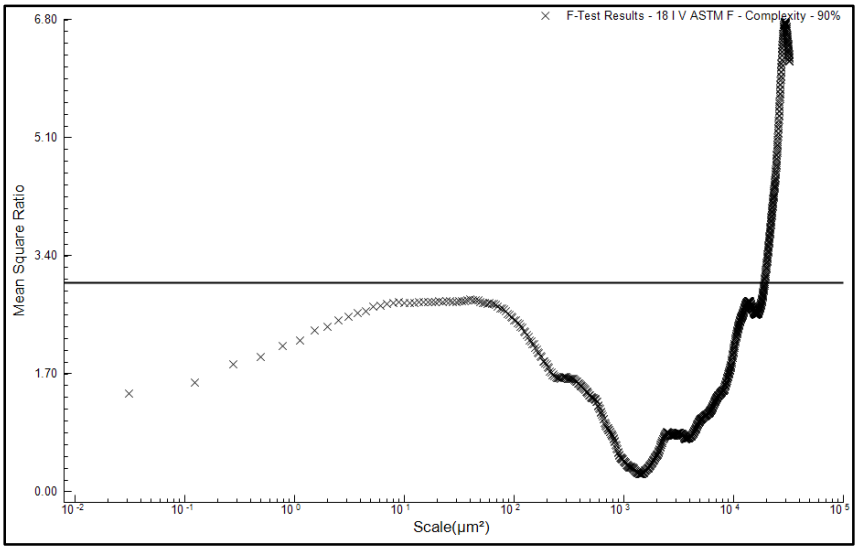

Figure 47: 18 Iron Surface against ASTM Front Side Surface

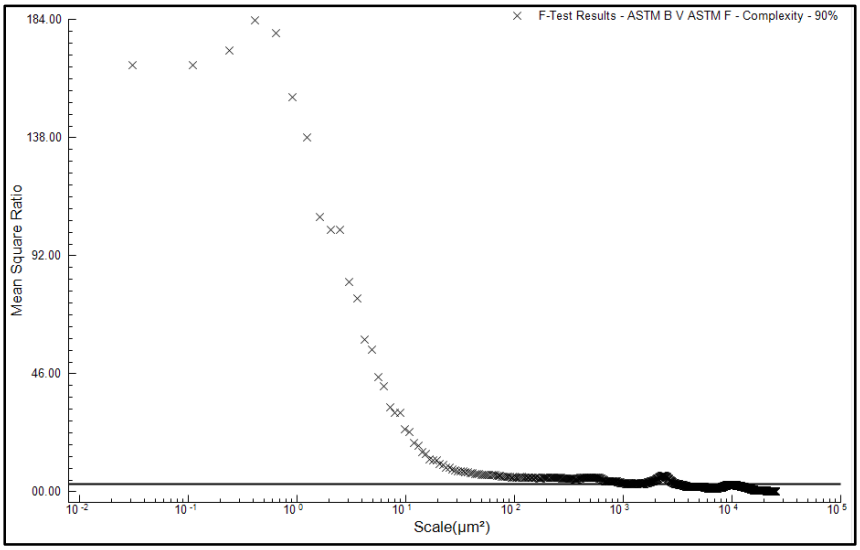

Figure 48: ASTM Back Side Surface against ASTM Front Side Surface

90% Confidence Interval F-Test for Material 2

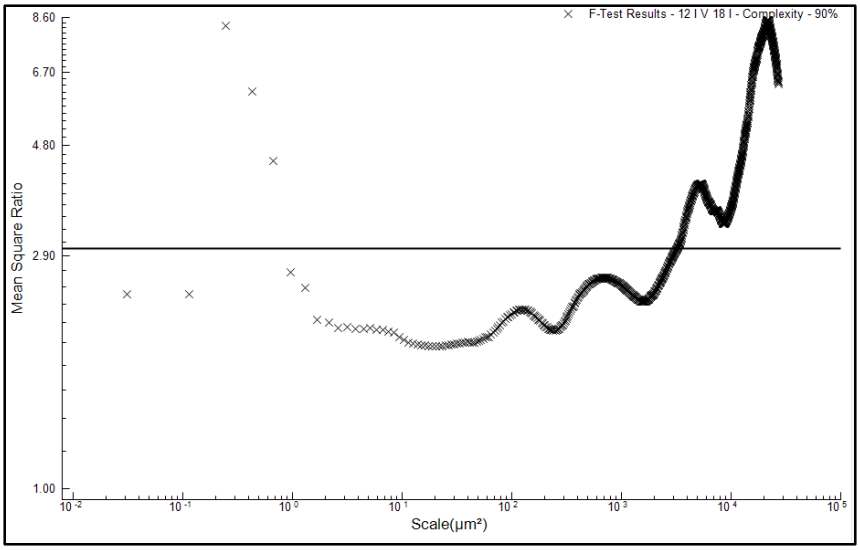

Figure 49: 12 Iron Surface against 18 Iron Surface

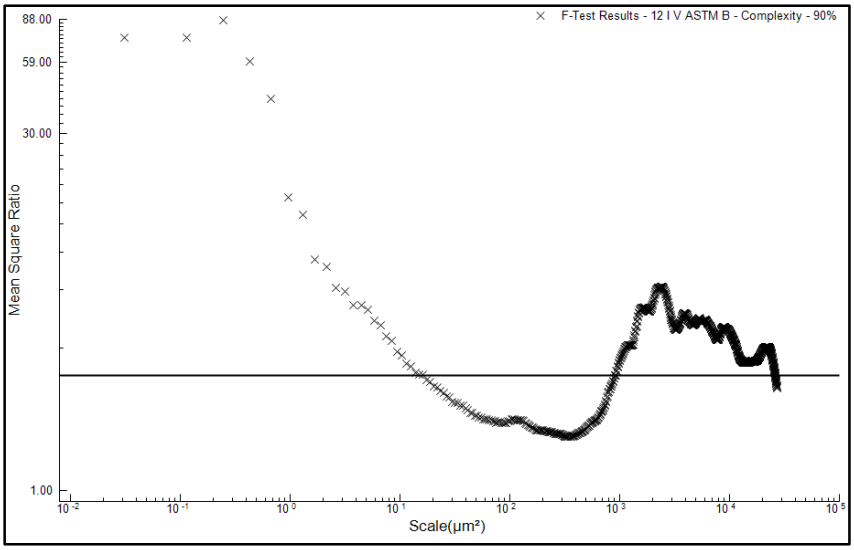

Figure 50: 12 Iron Surface against ASTM Back Side Surface

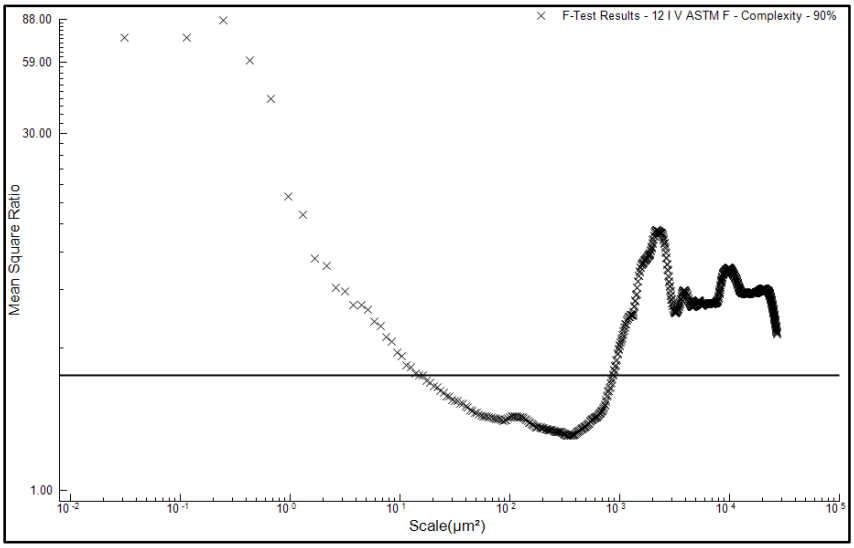

Figure 51: 12 Iron Surface against ASTM Front Side Surface

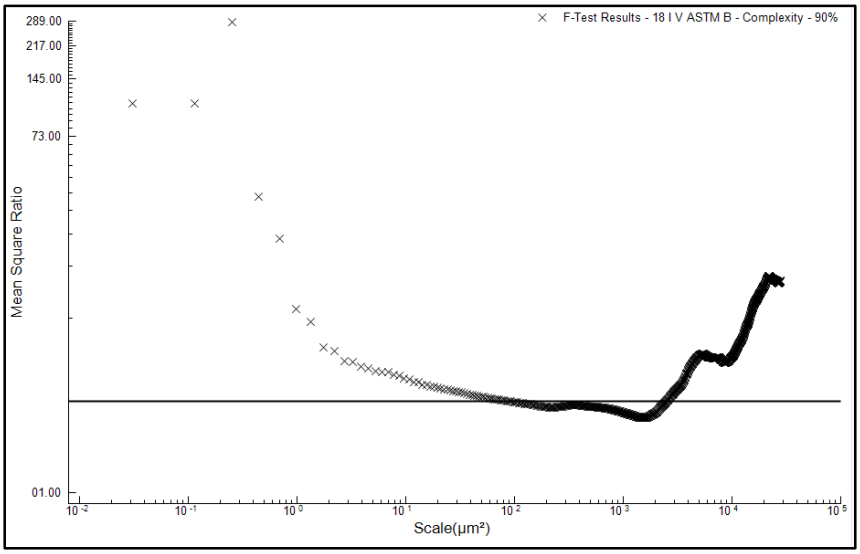

Figure 52: 18 Iron Surface against ASTM Back Side Surface

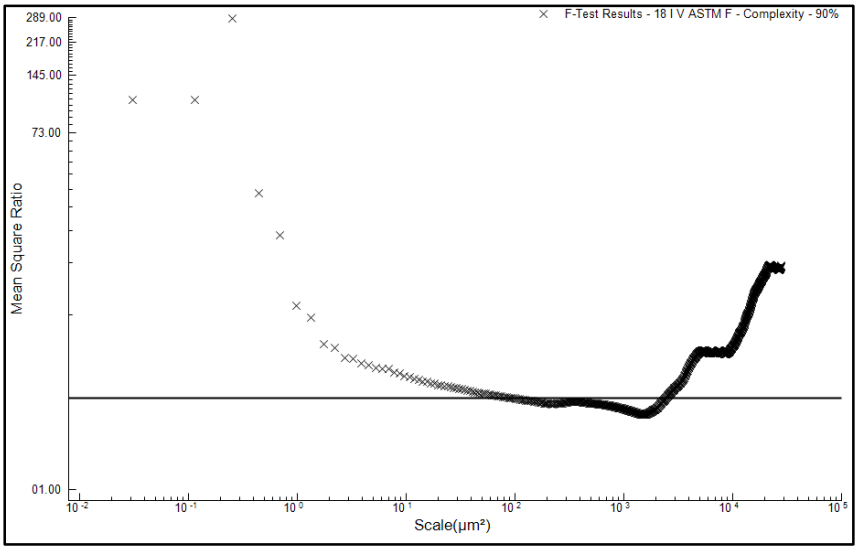

Figure 53: 18 Iron Surface against ASTM Front Side Surface

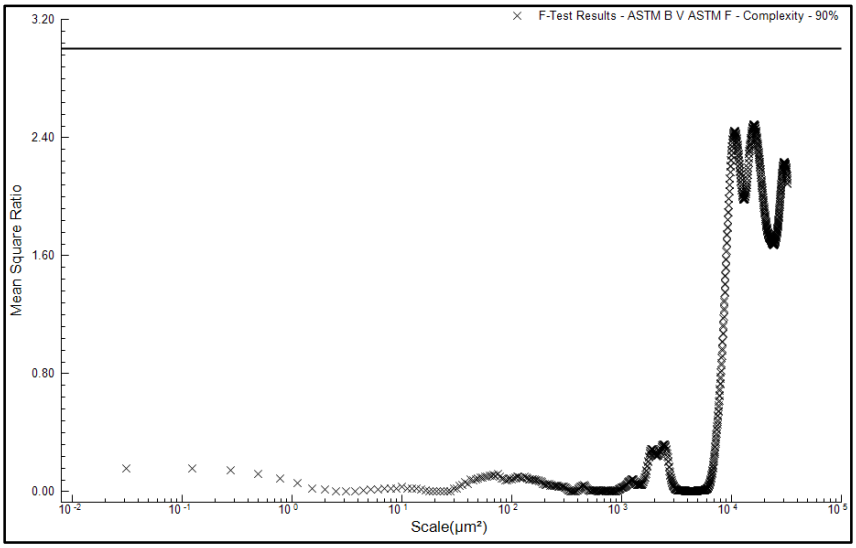

Figure 54: ASTM Back Side Surface against ASTM Front Side Surface

Appendix J

Testing Device Decomposition

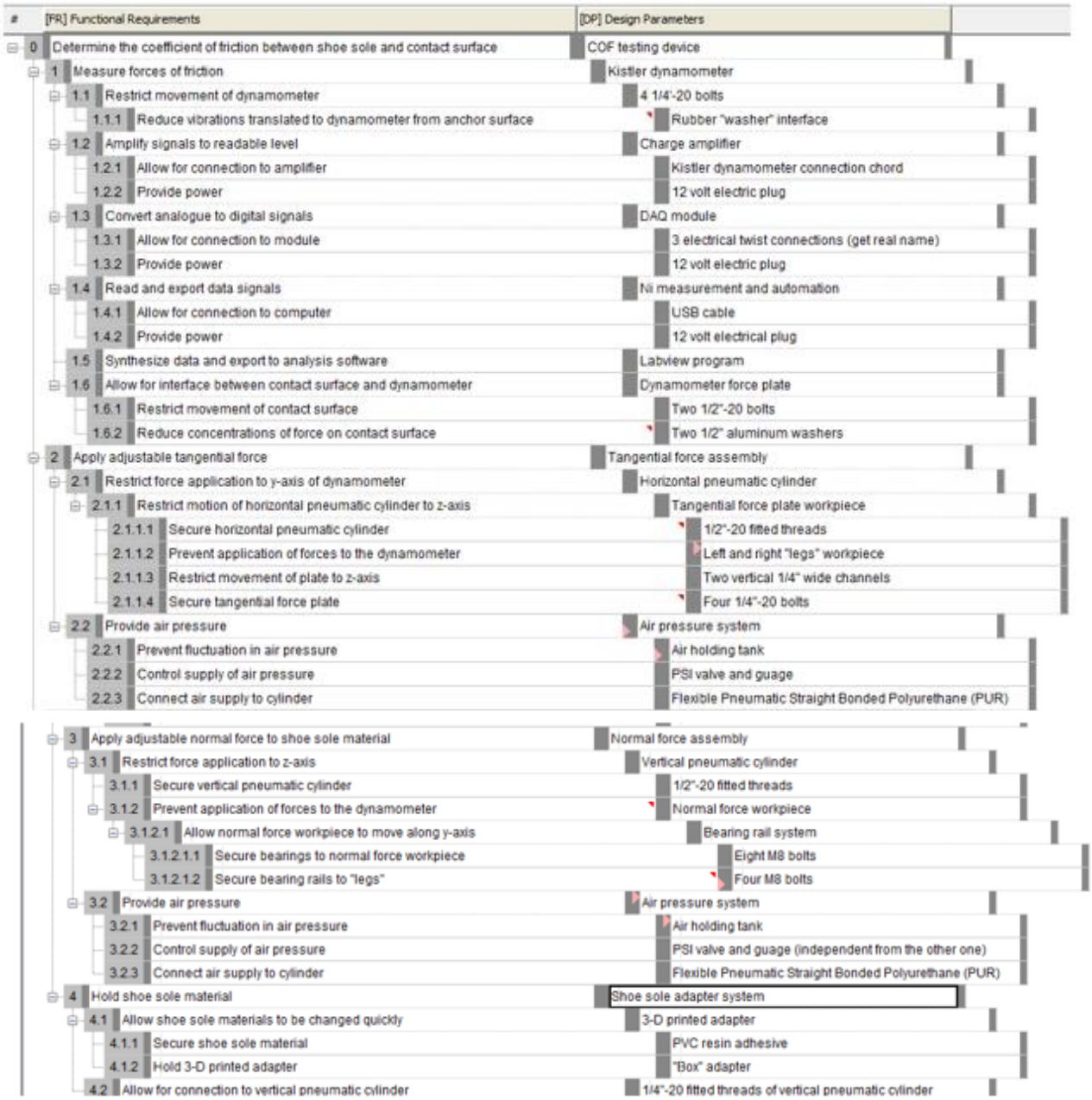

FR-0: Determine the coefficient of friction between shoe sole and contact surface

The primary objective of our testing apparatus is a simple one that requires two materials to be rubbed against each other and for those forces to be translated to the Kistler dynamometer. However,

the design can be complicated by the need to control the normal and tangential forces, control the movement of the two materials, and isolating the dynamometer from influences not related to the COF. To accomplish this the DP-0 was a COF testing device assembly.

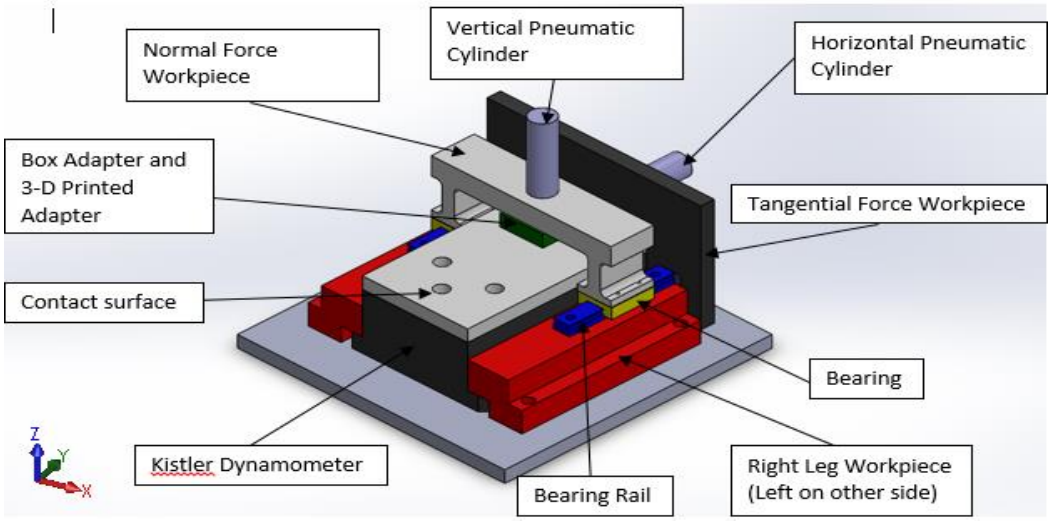

Figure 55: Components of Testing Device

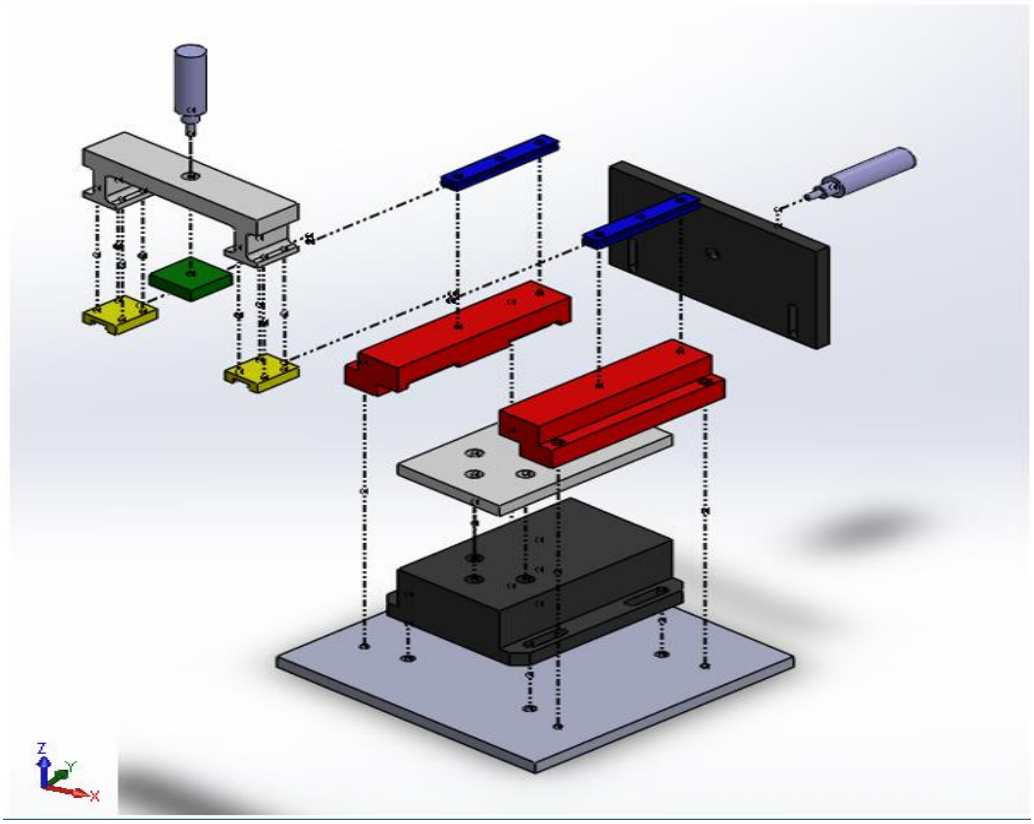

Figure 56: Exploded View of Testing Device Components

Part Name	Design Parameter Number
Kistler Dynamometer	1
Contact Surface	1.6.1
Horizontal Pneumatic Cylinder	2.1
Tangential Force Plate Workpiece	2.1.1
Left and Right Leg Workpieces	2.1.1.2
Vertical Pneumatic Cylinder	3.1
Normal Force Workpiece	3.1.2
3-D Printer Adapter	4.1
Box Adapter	4.1.2

FR-1: Measure forces of friction

In order to calculate the COF at any given time one must know the magnitude of the normal force and the tangential force needed to slide the materials across one another. To do this, and for reasons stated in the methods, the Kistler dynamometer was chosen as DP-1.

FR-1.1: Restrict movement of the dynamometer

To be as accurate as possible the dynamometer cannot move throughout the duration of COF testing. To secure the device DP-1.1, four ¼''-20 bolts, was developed. These bolts could be used to secure the dynamometer to a variety of materials.

FR-1.1.1: Reduce vibrations translated to dynamometer from anchor surface

During initial use and calibration of the dynamometer it was clear that it was sensitive enough to pick up vibrations caused rolling around in a chair, or dropping a pen on the workbench. To combat the collection of any data not stemming from the COF test a rubber washer interface was used, which is DP-1.1.1. The washer was comprised of old bike tire inner tubes that would help mitigate any vibrations or forces being translated to the dynamometer via the workbench.

FR-1.2: Amplify signals to readable level

The output electrical signal of the dynamometer is very low, low enough that the data acquisition equipment would not be able to read it. Therefore the signal would need to be amplified. DP-1.2 was a Kistler charge amplifier.

Connecting the two is vital because our data acquiring DAQ box and software cannot process the output of the dynamometer

FR-1.2.1: Allow for connection to amplifier

The kistler dynamometer has a type 1687B5 cable output connection, while the charge amplifier has a type 1688B5 cable input connection. To connect the two devices a Kistler type 1689B5 connection cord was used that is meant specifically for this model of dynamometer and corresponding charge amplifier. This cord is DP-1.2.1.

FR-1.2.2: Provide power

The type 5004 dual mode amplifier required a 12-volt power source. The corresponding DP (1.2.2) was a 3-prong 12 volt electric plug.

FR-1.3: Convert analogue signal to digital signals

The output signal of the type 5004 dual mode amplifier is analogue. In order to collect and process any data coming from the dynamometer the output signal would have to be converted to digital. The corresponding DP to fulfill this requirement is the National Instruments 16-bit DAQ box, which is commonly used throughout the engineering community for data acquisition.

FR-1.3.1: Allow for connection to module

The charge amplifier has three output connections, one each of the 3 axes it can measure along. These connections are meant for bnc connectors, the same as the input connections for the DAQ module. DP-1.3.1 is three bnc connection cords.

FR-1.3.2: Provide power

THe DAQ module also requires a 12 volt power source. DP-1.3.2 is a 3 prong 12 volt electrical plug. This was an independent plug from the one used in DP-1.2.2.

FR-1.4: Read and export data signals

At this point in the decomposition there is a digital signal that is available to be read and measured. The corresponding DP for this functional requirement is Ni measurement and automation.

FR-1.4.1: Allow for connection to computer

In order to use the Ni measurement and automation our group had to use a WPI computer and server. Therefore, the corresponding DP-1.4.1 was developed so that it could be connected via a USB cable.

FR-1.4.2: Provide Power

FR-1.5: Synthesize data and export to analysis software

The Kistler dynamometer and the DAQ module do not come with a specific analysis software and there is no specific software, that we had access to at least, designed for our equipment and needs. Therefore, when developing DP-1.5, we were able to reference a class our team had taken earlier in our academic careers. Engineering experimentation taught us how to use a program called LabView, which allows one to design a operating analysis "software" based on their needs. This program was chosen as our design parameter.

FR-1.6: Allow for interface between contact surface and dynamometer

In this project the contact surface is a constant, in our case a aluminum plate having a surface roughness that would not change from test to test. To translate the forces of friction to the dynamometer this plate would need to be secured to it. The dynamometer force plate, which is DP-1.6, has pre-drilled and tapped ½''-20 holes.

FR-1.6.1: Restrict movement of contact surface

DP-1.6.1 was developed to be two ½''-20 bolts to fit in the pre-existing ½''-20 bolt holes in the force plate.

FR-1.6.2: Reduce concentrations of force on contact surface

Aluminum is a soft metal and if any other contact surface material was used, such as a ceramic, the concentration of force applied by the bolt head could alter the surface, warp, or break the material. DP-1.6.2 are two ½'' aluminum washers.

FR-2: Apply adjustable tangential force

As tangential force is one of the two forces that go into calculating the COF, the testing apparatus had to be able to this force at a designated place. The DP to accomplish this FR is the tangential force assembly.

FR-2.1: Restrict force application to y-axis of dynamometer

For testing purposes it was important that the force be applied only along the y-axis to prevent any unwanted moments. It was also important that the force could be applied along the y-axis, at any given point. To fulfill this FR the DP-2.1 of a horizontal pneumatic cylinder was developed.

FR-2.1.1: Restrict motion of horizontal pneumatic cylinder to z-axis

First, in order to apply a force along the y-axis with the pneumatic cylinder there is a need for a material to secure it to. Secondly, if a different contact surface was ever needed and had a different thickness then the tangential force would need to be applied at a different point on the z-axis. To accomplish these two needs DP-2.1.1 a tangential force plate workpiece was.

FR-2.1.1.1: Secure horizontal pneumatic cylinder

As mentioned previously, the testing apparatus must hold this cylinder in a fixed position. DP 2.1.1.1 is a ½''-20 fitted threads through the tangential force plate workpiece as the pneumatic cylinder comes already machined with ½''-20 threads.

FR-2.1.1.2: Prevent application of forces to the dynamometer

To obtain data from the dynamometer that are only from a COF testing the tangential force plate workpiece could not come into contact with the dynamometer force plate. To accomplish this task the design parameter of left and right "legs" workpiece were developed. DP-2.1.1.1 was developed as a way to integrate the horizontal tangential force plate workpiece into an assembly that went around and was completely independent of the dynamometer.

FR-2.1.1.3: Restrict movement of plate to z-axis

As the horizontal pneumatic cylinder is secured to the plate, the plate must therefore move along the z-axis. By machining two vertical ¼'' wide channels on either side the plate can be secured to whatever assembly while still be able to slide up and down. The channels are DP-2.1.1.3.

FR-2.1.1.4: Secure tangential force plate

The plate must also be secured to a solid workpiece as it must withstand the forces that the pneumatic cylinder will be producing. DP-2.1.14 are four ¼''-20 bolts and fitted threads in the left and right legs workpieces.

FR-2.2: Provide air pressure

The pneumatic cylinders are designed to operate by pressurizing air inside the device which pushes the piston out. A air pressure system was developed for the corresponding DP 2.2.

FR-2.2.1: Prevent fluctuation in air pressure

Any fluctuation of air pressure affects the amount of force that is being applied by the pneumatic cylinders piston. If our team were to use the large system that supplies an entire lab and can be used by others at the same time we risk having air pressure fluctuations at any time. Therefore DP 2.2.1 is an air holding tank that can be filled from the system described above, but can be made independent with the twist of a valve.

FR-2.2.2: Control supply of air pressure

The air system was capable up pressurizing the tank to just above 100 psi. This pressure could not be applied to the pneumatic cylinder all at once however. In order to control the air pressure DP-2.2.2 was developed to be a air valve and PSI gauge.

FR-2.2.3: Connect air supply to cylinder

To supply the air pressure from the valve to the pneumatic cylinder a connection line was needed that could handle the maximum pressure. The connection line also had to be flexible in order to move with the testing apparatus but be stiff enough to retain its shape while under pressure. If the line is too flexible it can result is a variation in air pressure. DP-2.2.3 was developed as a flexible pneumatic straight bonded polyurethane line.

FR-3: Apply a adjustable normal force to shoe sole material

Just as the tangential force assembly provided a means of moving the shoe sole material along the y-axis of the dynamometer, to calculate a COF a means of applying a normal force is also needed. DP-3 is a normal force assembly.

FR-3.1: Restrict force application to z-axis

It was very important that the applied normal force had to ability to, and only moved along the z-axis. The corresponding DP is the vertical pneumatic cylinder.

FR-3.1.1: Secure vertical pneumatic cylinder

In order to apply or normal force the cylinder would need to be secured. DP 3.1.1 is ½''-20 fitted threads.

FR-3.1.2: Prevent application of forces to the dynamometer

Again the dynamometer had to be kept independent from any forces being applied unless that force was pushing down on the shoe sole material. To accomplish this task DP-3.1.2 of a normal force workpiece was developed.

FR-3.1.2.1: Allow normal force workpiece to move along y-axis

During the duration of a COF test the shoe sole material would have to slide across the dynamometer. During that movement the normal force must remain constant or the COF will be affected. This means that the normal force workpiece, along with the pneumatic cylinder, would also have to move along the y-axis. The corresponding DP for this functional requirement was a bearing rail system.

FR-3.1.2.1.1: Secure bearings to normal force workpiece

In order to secure the bearings to the normal force workpiece the eight M8 bolts that came with the system had to be used. The bolts are DP-3.1.2.1.1.

FR-3.1.2.1.2: Secure bearing rails to “legs”

The other half of the system would then need to be secured to a material independent of the dynamometer. As the left and right leg workpieces are already serving that purpose they were to be that material. DP-3.1.2.1.2 was developed as the four remaining M8 bolts that came with the system.

For FR-3.2.1 to 3.2.3 please refer to FR-2.2.1 to 2.2.3 as they are the same functional requirements. At this time in the decomposition of the design there is one DP pairing. The air holding tank is the same

tank that is used to provide the air pressure to the horizontal pneumatic cylinder. This could be avoided by using another, separate air tank. The PSI valve and gauge, as well as the flexible pneumatic straight bonded polyurethane were independent of the previously stated DP's.

FR-4: Hold shoe sole material

The last requirement of the COF testing device was to be able to control the shoe sole material. Applying the normal and tangential force using only the piston of the pneumatic cylinder would cause the pliable rubber polymers to bend and warp. It would also cause force concentrations that could affect our data. A shoe sole adapter system was developed as DP-4.

FR-4.1: Allow shoe sole materials to be changed quickly

The only way to achieve even force distribution would be by applying the force through a flat plate the same size as the rubber polymer face it is in contact with. For testing purposes however there was a functional requirement that the team be able to change the shoe sole material quickly and easily. We therefore developed DP4.1, a 3-D printed adapter piece.

FR-4.1.1: Secure shoe sole material

To secure the material to the adapter piece an adhesive was chosen as it would secure the entire area of the polymer, compared to a screw that would warm and alter the surface. DP-4.1.1 was chosen to be a PVC two-part resin adhesive that was safe to use on the rubber polymer.

FR-4.1.2: Hold 3-D printed adapter

As the shoe sole material was secured to the adapter piece there was still a functional requirement to hold, or control, the movement of the two materials. To accomplish this a aluminum "box" adapter was developed. The box adapter is DP-4.1.2.

FR-4.2: Allow for connection to vertical pneumatic cylinder

The last step of this design decomposition was to ensure that the box adapter could be attached to the vertical pneumatic cylinder. This was important so that there was no slipping between the piston and the box adapter throughout the duration of the test. The corresponding DP are ¼''-20 fitted threads of the vertical pneumatic cylinder.

2. Prototype Production

In order to produce the workpieces, our team had to machine each part using a HAAS Minimill. The manufacturing of the workpieces required the HAAS Minimill to ensure that they were as accurate as possible to the predetermined measurements. All of the workpieces were created from 6061-T6 Aluminum stock. This material was chosen because of it is inexpensive compared to other materials and can be easily machined. The material is also strong enough to withstand the largest magnitude of forces that the testing apparatus could apply.

Each workpiece was first designed using the SolidWorks program. Once completed the SolidWorks part was imported into the machining program ESPRIT. The appropriate tooling information and tooling paths were inputted into the program to produce the desired features of the stock material.

DP-2.1.1: Tangential Force Plate Workpiece

To machine this workpiece a 8'' x 6'' x ¼'' stock was ordered. To reduce the amount of milling needed the stock was cut with a bandsaw so it was just over the desired width. The minimill was programed to machine any extra material on the left or right side to achieve the desired length, and then to machine the two slots all the way through the stock. This can be seen below.

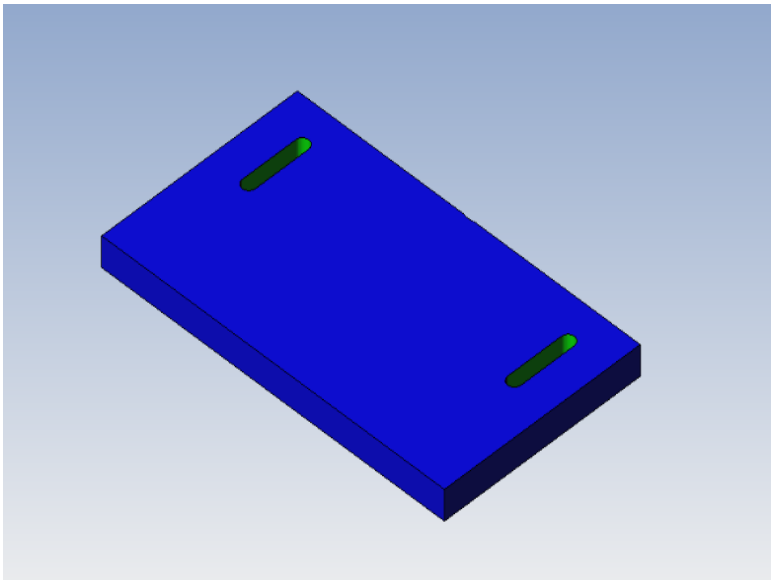

Figure 57: Testing Device Tangential Force Plate Workpiece

The workpiece was then orientated differently within the vice grips of the minimill. This allowed the program to mill any extra material on the front or back of the workpiece to ensure the desired dimensions were met. The final step was to drill the hole at the desired location. The tapping of the hole in order to secure the horizontal pneumatic cylinder was done by hand. It is shown below.

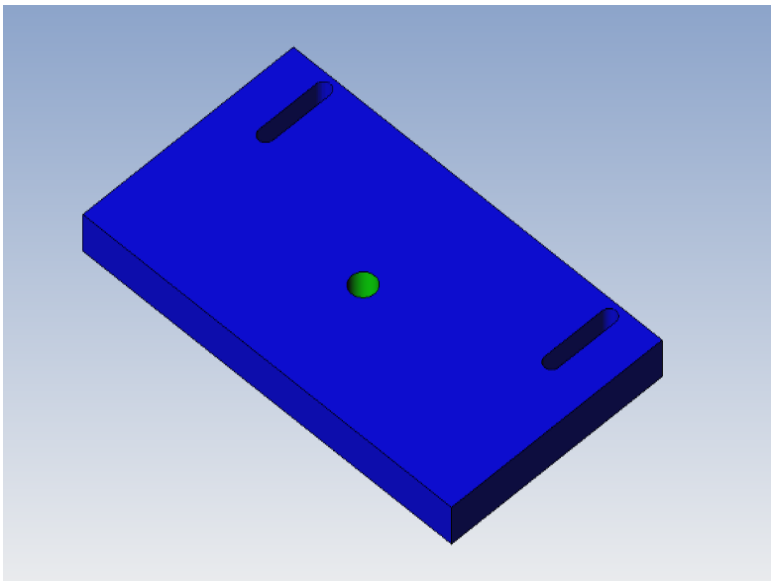

Figure 58: Testing Device Tangential Force Plate Workpiece with center hole

DP-2.1.1.2: Left and Right Leg Workpieces

Both the left and right leg workpieces were identical parts so the program and process to machine both were the same. The stock material was cut with a bandsaw just over the desired length. The first step was to remove enough material so that a ¼''-20 bolt could reach the workbench underneath. This was done by milling as well as drilling a clearance hole for the head of the bolt and can be seen below. Lastly the minimill was programmed to remove any excess material on either side so the desired length was achieved.

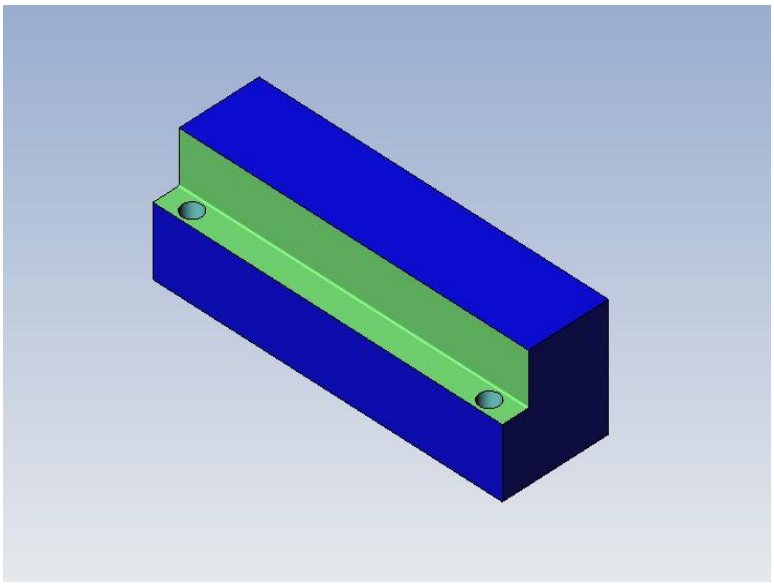

Figure 59: Left Leg Workpiece

The stock was then flipped over so it could be faced down to the desired height and the remaining features could be milled. The last step was to complete the through hole that allows the bolt to reach the workbench. These operations are shown below.

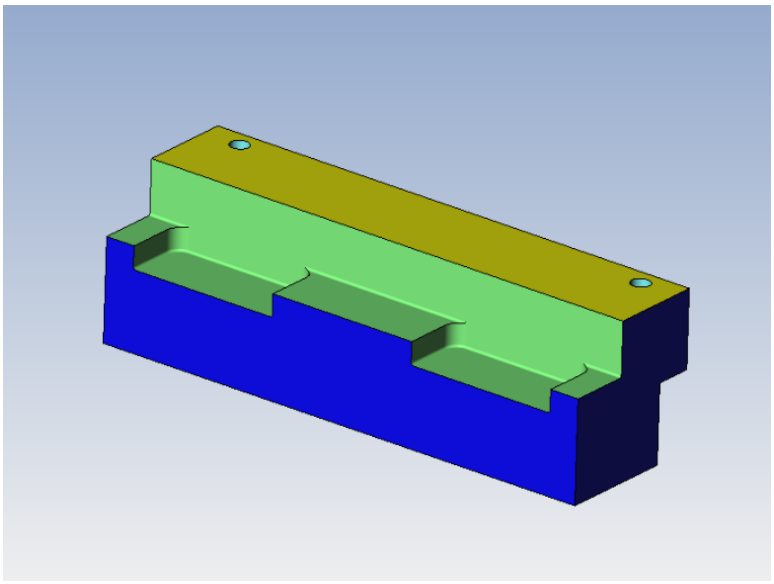

Figure 60: Right Leg Workpiece

While the process of drilling and tapping three ¼''-20 bolt holes were done in ESPRIT, in an effort to reduce time, and because these hole did not have to be exact, they were done by hand. This is also the only feature that was not exactly the same for the left and right leg workpieces. The holes were drilled on opposite sides of each other respectively so the tangential force workpiece has something to be secured to on both sides of the dynamometer. The ESPRIT file is shown below.

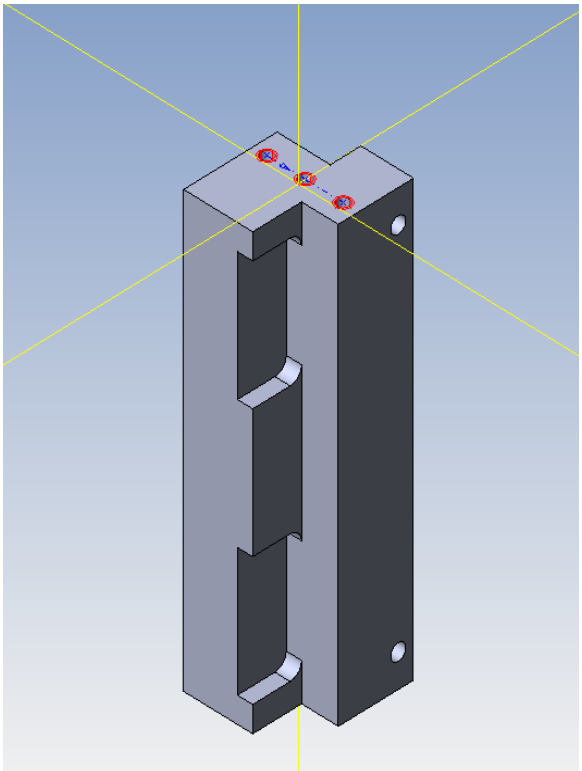

Figure 61: Left Leg ESPIRIT File

DP-3.1.2: Normal Force Workpiece

After the stock material was loaded into the vice grips of the minimill it was programmed to mill the following features into the workpiece. The tool used to accomplish this was not long enough to reach the bottom of the part however. Step one is shown below.

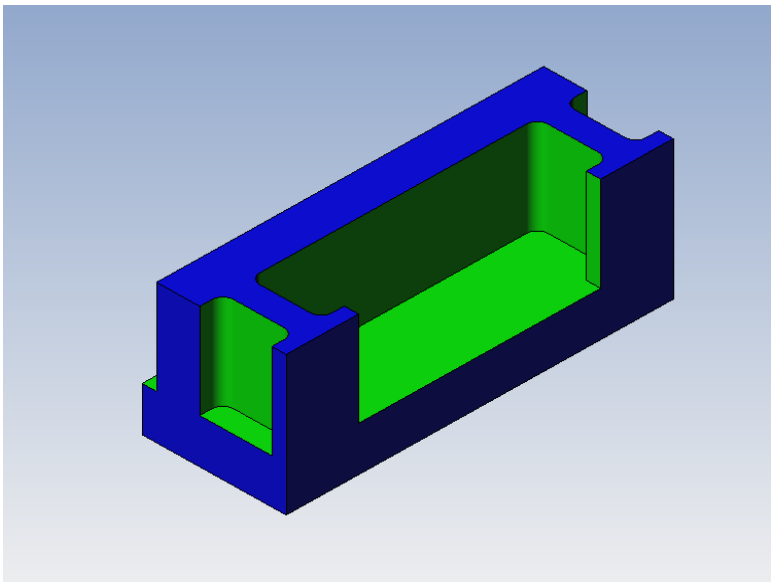

Figure 62: Normal Force Workpiece

The stock was then flipped over and machined down to the desired height as shown below.

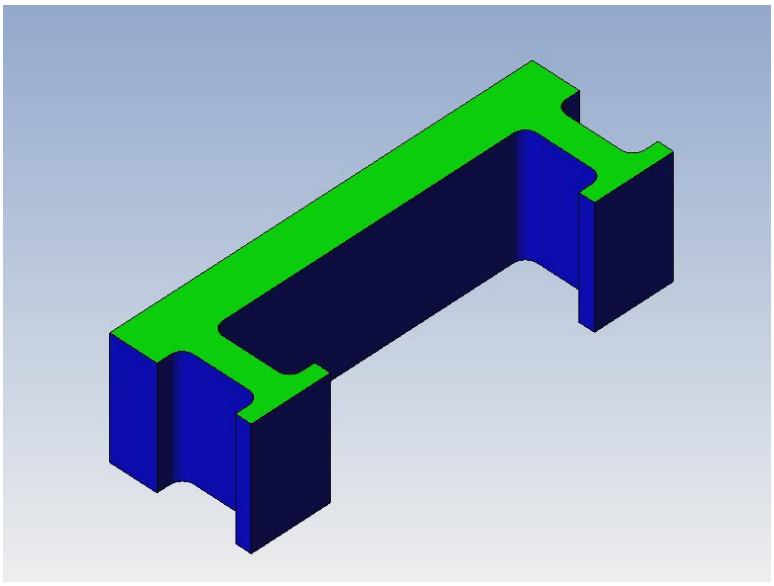

Figure 63: Normal Force Workpiece

Similar to the left and right leg workpieces the hole in the top of the part shown below was drilled and tapped by hand.

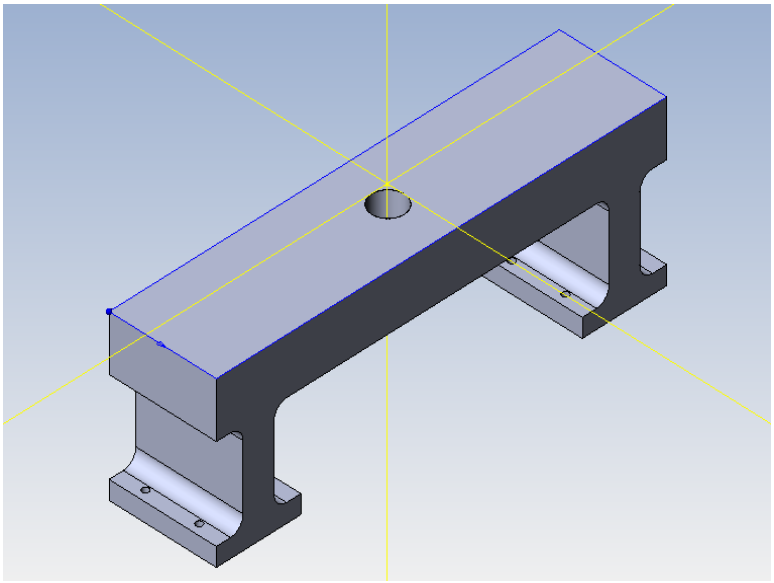

Figure 64: Espirit File for Normal Force Workpiece

DP-4.1.2: Box Adapter

The box adapter part was used from a previous MQP done here as WPI. The only difference between this figure from when the previous group machined the part and ours is that we drilled a ¼''-20 hole in the center in order to allow the pneumatic piston to attach to it.

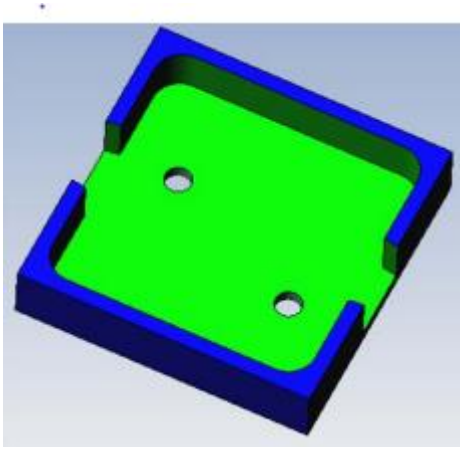

Figure 65: Box Adapter